



OPEN

# Intermittent hypoxia-induced enhancements in corticospinal excitability predict gains in motor learning and metabolic efficiency

Alysha T. Bogard<sup>1</sup>, Thomas G. Hembree<sup>1</sup>, Aviva K. Pollet<sup>1</sup>, Andrew C. Smith<sup>2</sup>,  
Stephanie C. Ryder<sup>2,3</sup>, George E. Marzloff<sup>2,3</sup> & Andrew Q. Tan<sup>1,3,4</sup>✉

Acute intermittent hypoxia (AIH) enhances human motor function after incomplete spinal cord injury. Although the underlying mechanisms in humans are unknown, emerging evidence indicates that AIH facilitates corticospinal excitability to the upper limb. However, the functional relevance of this plasticity remains unexplored, and it is unclear whether similar plasticity can be induced for lower limb motor areas. We recently demonstrated that AIH improves motor adaptation, motor savings, and metabolic efficiency during split-belt walking. Thus, we hypothesized that AIH increases lower limb excitability and that these enhancements would predict the magnitude of motor learning and the corresponding reductions in net metabolic power. We assessed tibialis anterior (TA) excitability using transcranial magnetic stimulation and quantified changes in spatiotemporal asymmetries and net metabolic power in response to split-belt speed perturbations. We show that AIH enhances TA excitability, and that the magnitude of this facilitation positively correlates with greater spatiotemporal adaptation. Notably, we demonstrate a novel association between increased excitability and reduced net metabolic power during motor adaptation and motor savings. Together, our results suggest that AIH-induced gains in excitability predict both the magnitude of motor learning and the associated metabolic efficiency. Determining indices of AIH-induced improvements in motor performance is critical for optimizing its therapeutic reach.

Acute intermittent hypoxia (AIH), involving brief alternating exposures to low-oxygen air, shows promise as an adjuvant to conventional locomotor training to enhance motor function following a motor incomplete spinal cord injury (iSCI)<sup>1–3</sup>. Despite considerable research in rodents<sup>4,5</sup>, the neural mechanisms underlying gains in motor performance remain unclear in humans. Both animal<sup>6</sup> and human studies<sup>7</sup> suggest that AIH induces neuroplastic changes that prime the nervous system for further improvements in motor function with neurorehabilitation training. Understanding the neurophysiological underpinnings of AIH-induced plasticity and its functional significance is critical to optimize its therapeutic reach.

One potential mechanism underlying AIH-induced gains in motor performance is enhanced excitability of residual descending motor pathways. Motor-evoked potentials (MEPs) elicited by transcranial magnetic stimulation (TMS) reflect the net excitability of intracortical and transcortical networks synapsing onto corticospinal neurons, including the contribution of various sensory relays from thalamocortical input<sup>8</sup>. Previous studies in able-bodied individuals have shown that AIH may facilitate corticospinal excitability (CSE) to the upper limb<sup>9,10</sup>. However, contrasting evidence indicates that prolonged hypoxic exposures do not alter CSE<sup>11</sup>, and milder single-session exposures either affect different TMS indices of CSE<sup>9,10</sup> or show no changes<sup>12</sup>. These discrepancies underscore a critical gap in our understanding of AIH-induced plasticity, including uncertainties regarding how repetitive AIH may differentially affect lower limb motor areas that support locomotor control. While our recent work found increased voluntary activation of ankle muscles after repetitive AIH<sup>13</sup>, it remains unclear whether CSE is elevated after repetitive AIH or how increased CSE influences motor performance.

Our recent study demonstrated that AIH enhances spatiotemporal adaptation during a novel split-belt walking task, suggesting that AIH may mediate motor performance through processes involved in motor adaptation and motor savings<sup>14</sup>. Such enhancements may be attributed to brain-derived neurotrophic factor

<sup>1</sup>Sensorimotor Recovery and Neuroplasticity Lab, Department of Integrative Physiology, University of Colorado, Boulder 80309, USA. <sup>2</sup>Department of Physical Medicine and Rehabilitation, University of Colorado School of Medicine, Aurora 80045, USA. <sup>3</sup>Rocky Mountain Regional VA Medical Center, Aurora 80045, USA. <sup>4</sup>Center for Neuroscience, University of Colorado, Boulder 80309, USA. ✉email: andrew.tan@colorado.edu

(BDNF)-dependent mechanisms, which have been shown to concurrently enhance CSE and facilitate various forms of motor learning, including sequence-specific<sup>15</sup> and visuomotor adaptation<sup>16,17</sup>. While the relationship between BDNF and motor adaptation is less well-defined, individuals with reduced BDNF levels due to a single-nucleotide polymorphism exhibit slower rates of motor adaptation during split-belt walking following stroke<sup>18</sup>. This suggests that parallels may exist between the mechanisms underlying motor adaptation and those supporting other forms of motor learning. Evidence from rodent models indicates that moderate AIH exposures increase motoneuron excitability through BDNF-dependent mechanisms<sup>4,5</sup>. Therefore, AIH-induced changes in CSE may reflect underlying plasticity mechanisms that drive gains in motor adaptation.

Human studies report positive correlations between elevated CSE and enhanced visuomotor adaptation<sup>19,20</sup>, while disrupting motor cortical processing through brief continuous theta burst stimulation reduces CSE and impedes retention<sup>21</sup>. Gains in CSE may relate to the challenge of the motor learning process itself<sup>22</sup> rather than specific movement parameters<sup>23</sup>. Assessing CSE to the tibialis anterior (TA) is clinically significant, as TA MEP amplitudes positively correlate with foot clearance during the swing phase of walking after iSCI<sup>24</sup> and TA EMG coherence strongly predicts split-belt motor adaptation in able-bodied individuals<sup>25</sup>. Electrophysiological evidence in humans indicates that corticospinal neurons form monosynaptic connections with TA motor neurons<sup>26,27</sup>. These synapses have been proposed as a primary site for AIH-induced neuroplasticity<sup>9</sup>, though subsequent work suggests that these neuroplastic effects may not consistently transfer to functional improvements<sup>28</sup>. Notably, TA excitability increases after novel skill training but not repetitive movement training<sup>29</sup> and is amplified during late stance of a precision target-matching walking task compared to regular walking<sup>30</sup>. Together, this evidence suggests that elevated CSE may serve as a marker of neuroplastic processes that promote motor learning. However, the correlation between changes in CSE and the magnitude of motor adaptation during a split-belt walking task is less well-defined.

Accordingly, this study investigated the effects of five consecutive days of AIH or SHAM treatment on TA excitability, motor adaptation, and motor savings. AIH involved 90-s intervals of breathing 9% ± 2% O<sub>2</sub> alternated with 60-s intervals of 21% ± 2% O<sub>2</sub> for 15 cycles<sup>3</sup>, whereas the SHAM group received blinded normoxia (i.e., SHAM; 21% ± 2% O<sub>2</sub>)<sup>31</sup>. We measured changes in resting TA excitability pre- and post-intervention using single-pulse TMS. To assess whether changes in CSE predict the magnitude of motor adaptation without any prior training, participants performed a split-belt walking task after the final AIH dose to eliminate the confound of task familiarity<sup>14</sup>.

We hypothesized that TA excitability would be enhanced following day five of AIH and that the magnitude of this change would predict both the extent of spatiotemporal adaptation during split-belt walking and motor savings of this adaptation. Since greater spatiotemporal adaptation is associated with decreased metabolic power<sup>32</sup>, with more pronounced reductions after AIH<sup>14</sup>, we further predicted a positive correlation between increased TA excitability and reduced net metabolic power. Bridging the gap between AIH-induced neuroplasticity and its functional significance is critical for maximizing the neurorehabilitative benefits of AIH.

## Results

### AIH increases lower limb excitability

The experimental design is summarized in Fig. 1A. Twenty-six able-bodied subjects participated in a pre-post study design to assess changes in CSE after 5 consecutive days of AIH ( $N = 13$ ) or SHAM ( $N = 13$ ). We generated recruitment curves by plotting the peak-to-peak MEP amplitudes against the normalized stimulus intensities based on the participant's resting motor threshold (RMT) (Fig. 1B)<sup>11</sup>. To assess changes in CSE, we quantified TMS-derived indices such as changes in the area under the recruitment curve, maximum MEP amplitude (MEP<sub>max</sub>), peak slope of the recruitment curve, and RMT.

The area under the recruitment curve was analyzed to assess global changes in CSE from 90 to 140% of RMT (Fig. 1C). A linear mixed-effect model, with fixed effects of timepoint (pre, post), group (AIH, SHAM), and their interaction, and a random intercept for participants, revealed a significant main effect of timepoint ( $F(1, 24) = 6.17, p = 0.020$ ). The main effect of group ( $F(1, 24) = 1.31, p = 0.264$ ) and the interaction between timepoint and group ( $F(1, 24) = 2.21, p = 0.150$ ) were not significant. Post-hoc comparisons showed that the area under the curve significantly increased from pre- to post-intervention in the AIH group (estimate = 0.528,  $SE = 0.188, p = 0.0098$ ), but not in the SHAM group (estimate = 0.132,  $SE = 0.188, p = 0.488$ ). In support of these findings, Wilcoxon signed-rank tests also showed a significant increase in the area under the curve for the AIH group ( $W = 13, p = 0.021$ ) but not the SHAM group ( $W = 50, p = 0.787$ ).

To further investigate changes in CSE, exploratory analyses of individual recruitment curve parameters, including MEP<sub>max</sub>, peak slope, and RMT, were conducted (Fig. 2). In the AIH group, MEP<sub>max</sub> significantly increased ( $W = 14, p = 0.027$ ), while peak slope ( $W = 25, p = 0.168$ ) and RMT ( $W = 44.5, p = 0.088$ ) did not change. Similarly, a repeated measures ANOVA comparing the MEP amplitude pre-AIH and post-AIH at the stimulus intensities of 100% RMT, 120% RMT, and 140% RMT, showed a significant main effect of both timepoint ( $F(1, 12) = 6.66, p = 0.024$ ) and stimulus intensity ( $F(1.18, 14.19) = 36.29, p < 0.001$ ) on MEP amplitude, as well as a significant interaction between timepoint and stimulus intensity ( $F(1.49, 17.86) = 4.79, p = 0.030$ ). Tukey's post-hoc comparisons indicated a significant increase in MEP amplitude from pre- to post-AIH for the stimulus intensities of 120% RMT ( $t(12) = -2.18, p = 0.050$ ) and 140% RMT ( $t(12) = -2.75, p = 0.018$ ). In contrast, the SHAM group showed no significant changes in MEP<sub>max</sub> ( $W = 35, p = 0.497$ ), RMT ( $t(12) = 0.85, p = 0.413$ ), peak slope ( $W = 26, p = 0.191$ ), or MEP amplitude at any RMT intensity level (no effect of timepoint ( $F(1, 12) = 0.02, p = 0.899$ ; effect of stimulus intensity ( $F(2, 24) = 16.77, p < 0.001$ , no interaction effect ( $F(2, 24) = 1.28, p = 0.296$ )).

Group comparisons of normalized MEP amplitudes (% baseline) highlighted significant differences. MEP<sub>max</sub> (% baseline) was significantly higher in the AIH group compared to the SHAM group ( $W = 132, p = 0.014$ ; Fig. 3A), with 9 out of 13 individuals showing elevated MEP<sub>max</sub> after AIH compared to baseline (independent

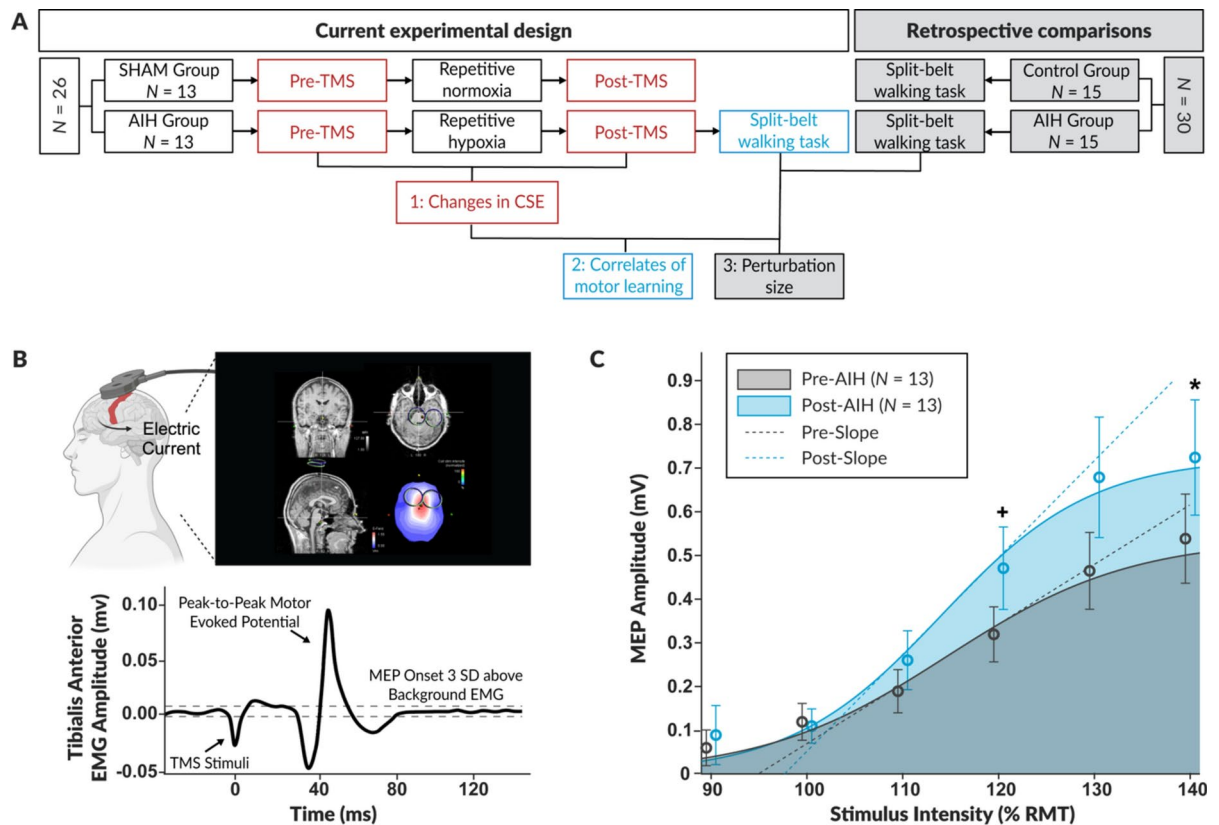


**Fig. 1.** Experimental design and recruitment curve. **(A)** Study overview. Twenty-six able-bodied participants were recruited for this study (AIH group  $N = 13$ ; SHAM group  $N = 13$ ). We assessed corticospinal excitability (CSE) to the tibialis anterior (TA) using transcranial magnetic stimulation (TMS) before intervention ('Pre-TMS') and after five consecutive days of AIH or SHAM ('Post-TMS'). To investigate correlations between changes in CSE and motor adaptation, participants in the AIH group performed a split-belt walking task. Retrospective comparisons included previously collected data (AIH group  $N = 15$ , Bogard *et al.*, 2023) to evaluate the influence of perturbation size (1:2 vs. 1:1.5 belt speed ratios) on motor adaptation. **(B)** TMS methodology. We applied single-pulse TMS over the scalp to target the lower limb motor area of the primary motor cortex. A neuronavigational system ensured trial-to-trial consistency in the stimulation vector. The hotspot corresponded to the location that elicited the lowest threshold and shortest latency motor evoked potential (MEP) amplitude. **(C)** AIH group recruitment curve. MEPs were recorded using surface electromyography (EMG) placed over the tibialis anterior muscle belly. We utilized the peak-to-peak MEP amplitude as an index to evaluate changes in corticospinal excitability, where the onset was identified as the first frame to exceed three standard deviations of the pre-stimulus background EMG. **(C)** The average recruitment curve for the AIH group ( $N = 13$ ) was generated by plotting the peak-to-peak MEP amplitude versus the normalized stimulus intensity based on 90% to 140% of the participants' resting motor threshold (RMT) pre-AIH (grey) and post-AIH (blue). The dashed line represents the Boltzmann slope, the shaded area depicts the area under the curve, and the bars represent standard error. The significance levels of an ANOVA comparing pre-AIH and post-AIH at the stimulus intensities of 100% RMT, 120% RMT, and 140% RMT are denoted as \* $p < 0.05$  and + $p = 0.05$ .

$t$ -test  $t(12) = 7.554$ ,  $p < 0.001$ ; Fig. 3B). These findings collectively demonstrate that TA excitability is enhanced on day 5 of AIH but not SHAM.

The TA EMG amplitude during maximal voluntary contractions did not change following AIH ( $t(12) = -0.78$ ,  $p = 0.450$ ) or SHAM ( $t(12) = 1.14$ ,  $p = 0.276$ ). These findings suggest that despite the observed increases in CSE following AIH, this did not translate into measurable changes in maximal voluntary motor output in able-bodied individuals. No participants were excluded outliers from the TMS analysis.

### Background EMG

Although CSE was assessed at rest, we evaluated the mean EMG signal recorded 200 ms preceding the TMS stimuli to ensure stable levels of pre-stimulus background EMG<sup>33</sup>. To further account for signal noise, background EMG was subtracted from all MEPs<sup>34</sup>. We did not observe any statistically significant differences in background EMG between pre-TMS and post-TMS sessions for the AIH group ( $t(12) = -0.72$ ,  $p = 0.486$ ) or the SHAM group ( $t(12) = -0.35$ ,  $p = 0.730$ ). This observation indicates that the variability in background EMG is not a significant factor contributing to any observed changes in the TA MEP amplitude pre- to post-intervention.

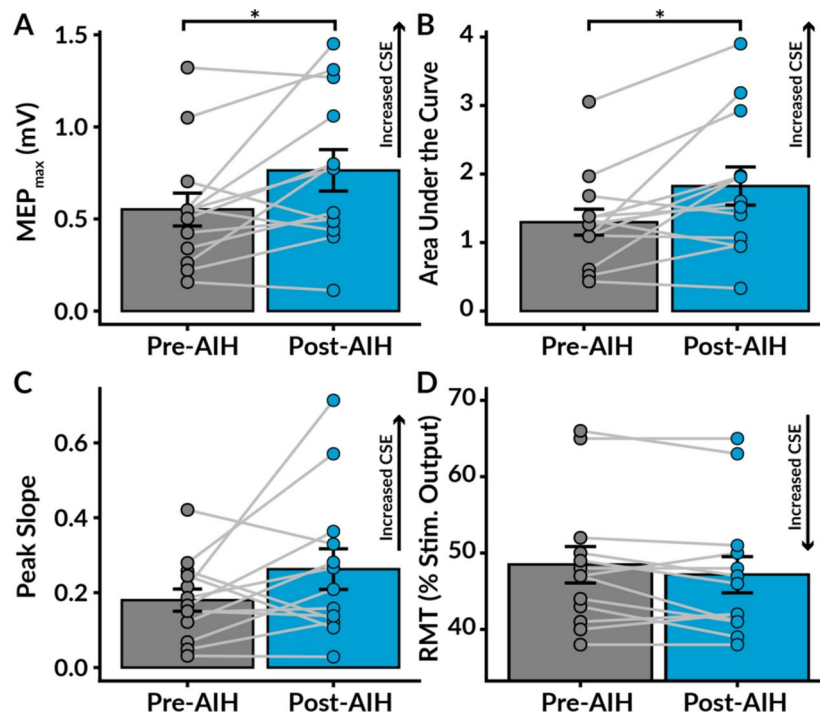


**Fig. 2.** Average corticospinal excitability pre- and post-acute intermittent hypoxia exposure. We evaluated changes in corticospinal excitability (CSE) pre- to post-acute intermittent hypoxia (AIH) by measuring alterations in the maximum motor evoked potential amplitude ( $MEP_{max}$ ), area under the recruitment curve, peak slope of the recruitment curve, and resting motor threshold (RMT; as a percent of the maximal stimulator output). **(A)** The average  $MEP_{max}$  significantly increased following AIH, indicating increased CSE. **(B)** The area under the recruitment curve, an index of net excitability from 90 to 140% of RMT, also significantly increased post-AIH. **(C)** There was no significant change in peak slope after AIH. **(D)** The RMT decreased after AIH but was not significantly different ( $p=0.088$ ). The bars represent standard error. Significance levels are denoted as \*\*\* $p<0.001$ , \*\* $p<0.01$ , and \* $p<0.05$ .

### Bayesian Hierarchical Modeling: MEP Amplitude and Background EMG

For the AIH group, Bayesian hierarchical modeling was used to examine the effects of timepoint (pre- vs. post-AIH) and background EMG on MEP amplitudes. Since the relationship between background EMG and MEP amplitude is not inherently linear, MEP amplitudes were log-transformed prior to analysis<sup>35</sup>. The model included fixed effects of timepoint and background EMG, as well as a random intercept for participant identifier to account for repeated measures.

Bayesian inference indicated a 97% posterior probability that AIH increases MEP amplitude ( $\beta=0.30$ , 95% credible interval (CI) [0.04, 0.54]). The evidence ratio (ER=29.77) suggests that the hypothesis of AIH increasing MEP amplitude is ~30 times more probable than the null hypothesis ( $\beta \leq 0$ ). Together, these results provide strong evidence that AIH increases MEP amplitude. In contrast, the posterior probability that background EMG has a positive effect was 56% ( $\beta=0.14$ , 95% CI [-1.46, 1.74]), with an ER of 1.25, providing weak and inconclusive evidence for an effect.

To further assess whether background EMG influenced MEP amplitudes, two Bayesian hierarchical models were compared using leave-one-out cross-validation (LOO-CV). One model included background EMG as a predictor (Model 1), while the other excluded it (Model 2). LOO-CV showed a small ELPD difference (-0.07, SE=0.2), indicating including background EMG did not improve predictive accuracy. Additionally, Bayesian  $R^2$  estimates indicated that both models explained similar variance in MEP amplitude (Model 1:  $R^2=0.865$ , 95% CI [0.701, 0.927]; Model 2:  $R^2=0.868$ , 95% CI [0.716, 0.928]), providing no evidence that including background EMG improved predictive performance.

Posterior predictive checks confirmed model fit, with  $\hat{R}=1$  for all parameters, indicating proper convergence, and ESS exceeding 1,000, ensuring robust posterior estimates. Together, these findings provide strong evidence that background EMG does not meaningfully contribute to the observed increase in MEP amplitude post-AIH.

### Motor adaptation: spatiotemporal asymmetry

We assessed motor adaptation in the AIH group by quantifying the extent of spatiotemporal adaptation from the first five strides ('initial learning') to the last twenty strides ('late learning') of two, 300-stride split-belt walking conditions, Adapt 1 and Adapt 2 (Fig. 4A–C). For both adaptation conditions, the perturbation was set at a 2:1 belt speed ratio. The spatiotemporal parameters of motor adaptation we analyzed included step length asymmetry (SLA), step time asymmetry (STA), and double support time asymmetry (DSA). Values that converged with the



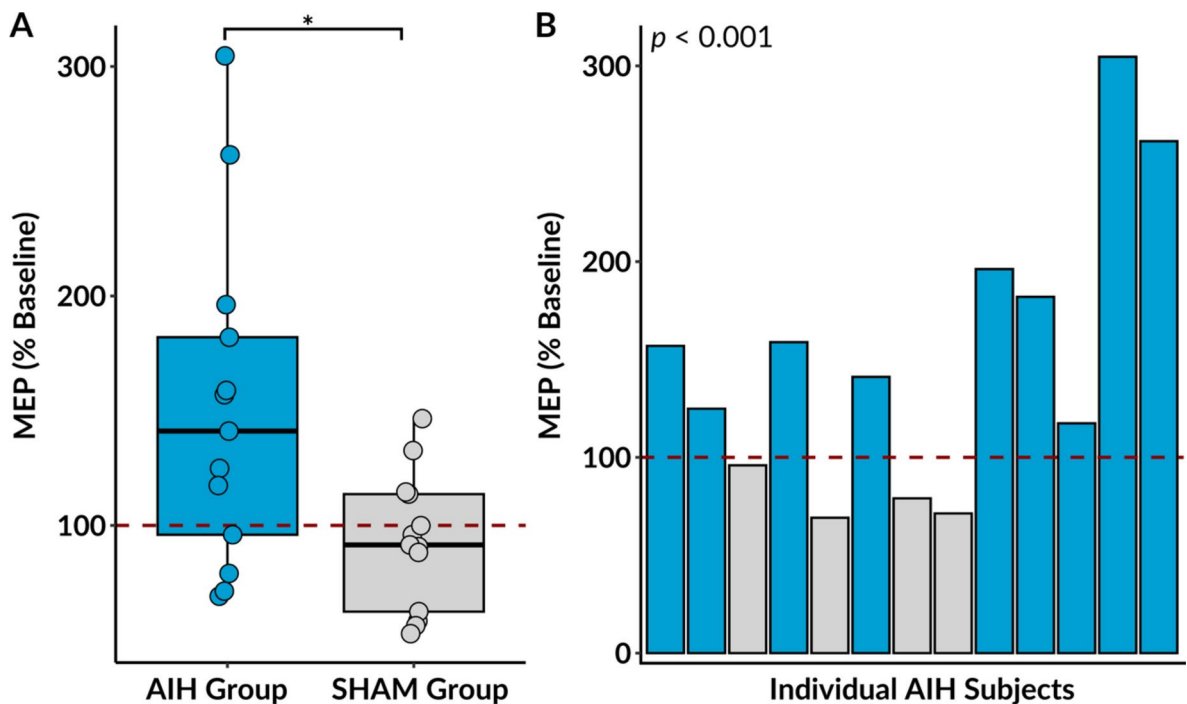


**Fig. 3.** Average corticospinal excitability as a percentage of baseline values following repetitive AIH versus repetitive SHAM. We assessed changes in maximum motor evoked potential amplitude ( $MEP_{max}$ ) relative to baseline (dotted red line at 100%) for both the acute intermittent hypoxia (AIH; blue) and blinded normoxia (SHAM; light grey) groups (**A**)  $MEP_{max}$  (% baseline) was significantly higher post-AIH compared to post-SHAM, indicating increased CSE only after AIH. Significance levels are denoted as  $*p < 0.05$ . (**B**) Individual variability in  $MEP_{max}$  changes on day 5 of AIH is shown as a percentage of baseline values. Each bar represents individual changes, with values above the dotted line indicating increased CSE post-AIH. The light grey bars indicate individuals who do not increase  $MEP_{max}$  post-AIH. An independent t-test shows MEP amplitude is significantly different than baseline MEP amplitude ( $p < 0.001$ ).

adaptation patterns extensively observed in able-bodied individuals reflected greater ‘learning’. Specifically, we characterized motor adaptation by reductions in SLA and DSA towards symmetry values of 0, coupled with augmentations in STA towards positive asymmetry<sup>37,38</sup>. One participant was excluded from all gait analyses due to utilizing a running strategy with a distinct aerial phase.

We found that participants adapted their interlimb coordination during Adapt 1 and Adapt 2 to minimize SLA and DSA, while STA remained high. A two-way ANOVA revealed significant main effects of both condition ( $F(1, 11) = 22.99, p < 0.001$ ) and learning phase ( $F(1, 11) = 36.15, p < 0.001$ ) on SLA, with a significant interaction between condition and learning phase ( $F(1, 11) = 15.43, p = 0.002$ ). Tukey’s post-hoc comparisons demonstrated a significant decrease in SLA from initial Adapt 1 to late Adapt 1 ( $t(11) = -5.65, p < 0.001$ ) and from initial Adapt 2 to late Adapt 2 ( $t(11) = -4.73, p < 0.001$ ). Conversely, for STA, a two-way ANOVA only observed a significant main effect of condition ( $F(1, 11) = 7.78, p = 0.018$ ). However, Tukey’s post-hoc comparisons did not indicate any significant changes in STA between initial Adapt 1 to late Adapt 1 ( $p = 0.214$ ), nor between initial Adapt 2 to late Adapt 2 ( $p = 0.784$ ). For DSA, a two-way ANOVA showed significant main effects of condition ( $F(1, 11) = 38.79, p < 0.001$ ) and learning phase ( $F(1, 11) = 14.89, p = 0.003$ ), with a significant interaction between the two ( $F(1, 11) = 6.82, p = 0.024$ ). Tukey’s post-hoc comparisons indicated a significant decrease in DSA from initial to late Adapt 1 ( $t(11) = -4.16, p = 0.002$ ) and initial to late Adapt 2 ( $t(11) = 2.21, p = 0.049$ ). These observations underscore the ability of able-bodied individuals to adapt spatial and temporal interlimb coordination in response to imposed gait asymmetries.

### Motor adaptation: net metabolic power

Given that spatiotemporal adaptations are paralleled by reductions in metabolic cost during split-belt walking<sup>14,32</sup>, we quantified concurrent changes in net metabolic power (W/kg) utilizing open-circuit spirometry. To account for the time lag of expired air reaching the mixing chamber, we quantified changes in ‘early’ and ‘late’ net metabolic power during the second and last minute of each condition, respectively (Fig. 4D)<sup>32</sup>.

An ANOVA detected significant main effects of condition ( $F(1, 11) = 9.76, p = 0.010$ ) and an interaction effect between condition and learning phase ( $F(1, 11) = 17.60, p = 0.001$ ). Tukey’s post-hoc comparisons identified a significant decrease in net metabolic power from early to late Adapt 1 ( $t(11) = 3.90, p = 0.002$ ) and from early to late Adapt 2 ( $t(11) = -2.47, p = 0.031$ ). Mean net metabolic power decreased from 6.09 W/kg during early Adapt 1 (SD = 1.51) to 5.73 W/kg during late Adapt 1 (SD = 1.32). Thus, as participants adapted their coordination, they simultaneously improved their metabolic efficiency.

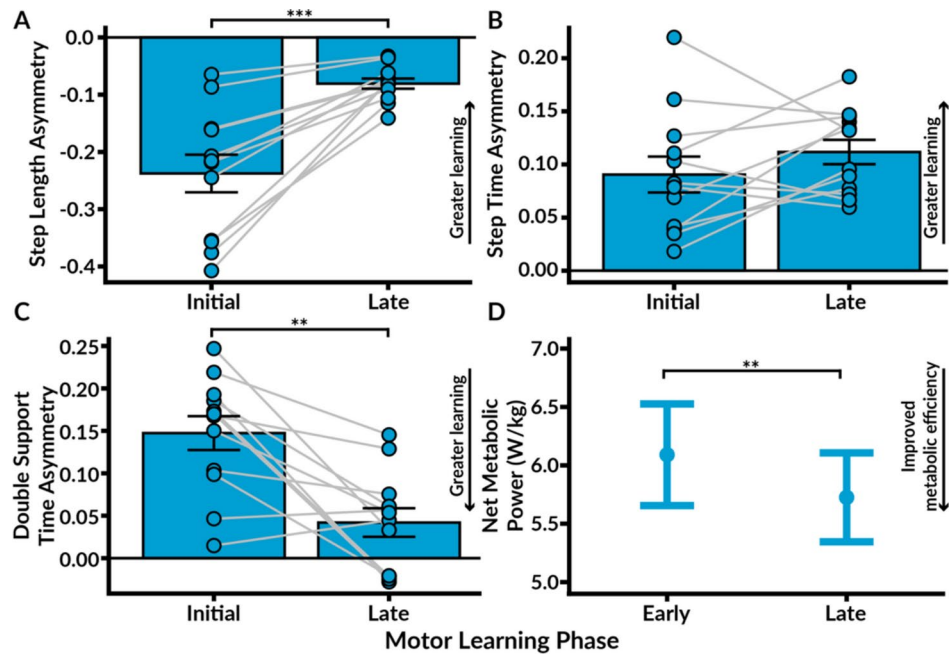


**Fig. 4.** Motor adaptation: Spatiotemporal and metabolic adaptation during the first exposure to split-belt walking. We quantified motor adaptation by measuring the extent of spatiotemporal adaptation from the first five strides ('initial') to the final twenty strides ('late') of the first exposure to split-belt walking ('Adapt 1'). Additionally, we assessed the magnitude of metabolic adaptation by comparing the second minute ('early') of Adapt 1 to the last minute ('late'). (A) We observed substantial reductions in step length asymmetry during Adapt 1, indicating spatial motor adaptation. (B) In contrast, step time asymmetry remained high without significant changes. (C) Double support time asymmetry significantly decreased from initial Adapt 1 to late Adapt 1, consistent with temporal motor adaptation. (D) Net metabolic power significantly reduced during Adapt 1, suggesting improved metabolic efficiency. The circles and light grey lines depict individual data. The bars represent standard error. Significance levels are denoted as \*\*\* $p < 0.001$ , \*\* $p < 0.01$ , and \* $p < 0.05$ .

#### Lower limb excitability predicts motor adaptation: spatiotemporal asymmetry

We performed linear regression analyses and calculated the adjusted  $R^2$  values to evaluate how well  $\Delta \text{MEP}_{\text{max}}$ ,  $\Delta$  area under the recruitment curve,  $\Delta$  peak slope, and  $\Delta$  RMT predicted the magnitude of motor adaptation (Fig. 5, Supplementary Table S1). We observed a significant positive correlation between increased  $\text{MEP}_{\text{max}}$  after AIH and reduced SLA during motor adaptation (Adjusted  $R^2 = 0.418$ ,  $p = 0.014$ ). Moreover, a positive trend emerged between elevated area under the recruitment curve after AIH and decreased SLA during motor adaptation (Adjusted  $R^2 = 0.256$ ,  $p = 0.053$ ). Stepwise linear regression identified both  $\Delta \text{MEP}_{\text{max}}$  and  $\Delta$  peak slope as the primary predictors of improved SLA during motor adaptation ( $\Delta \text{SLA} = 0.097 + 0.420 * \Delta \text{MEP}_{\text{max}} - 0.423 * \Delta$  peak slope,  $\text{AIC} = -65.29$ , model  $p = 0.039$ ,  $\text{MEP}_{\text{max}}$   $p = 0.032$ , peak slope  $p = 0.0395$ ), together explaining 56.72% of the variance.

Furthermore, we observed a significant positive correlation between increased  $\text{MEP}_{\text{max}}$  after AIH and higher STA during motor adaptation (Adjusted  $R^2 = 0.496$ ,  $p = 0.006$ ). The correlation between increased area under the recruitment curve after AIH and heightened STA (Adjusted  $R^2 = 0.189$ ,  $p = 0.088$ ) and the correlation between increased peak slope post-AIH and more positive STA (Adjusted  $R^2 = 0.233$ ,  $p = 0.064$ ) did not reach significance. Utilizing stepwise linear regression,  $\Delta \text{MEP}_{\text{max}}$ ,  $\Delta$  area under the recruitment curve, and  $\Delta$  RMT emerged as the best predictors of changes in STA during motor adaptation ( $\Delta \text{STA} = 0.015 + 0.245 * \Delta \text{MEP}_{\text{max}} - 0.071 * \Delta$  area under the recruitment curve  $+ 0.008 * \Delta$  RMT,  $\text{AIC} = -76.15$ , model  $p = 0.055$ ,  $\text{MEP}_{\text{max}}$   $p = 0.0297$ , area under the recruitment curve  $p = 0.120$ , RMT  $p = 0.194$ ), explaining 51.82% of the variance. Conversely, none of the TMS indices showed a significant correlation with decreased DSA during motor adaptation (model  $p = 0.967$ ). In summary, TMS indices reflecting changes in CSE after AIH significantly predicted the magnitude of motor adaptation observed for both SLA and STA.

#### Lower limb excitability predicts motor adaptation: net metabolic power

Interestingly, net metabolic power significantly correlated with  $\Delta \text{MEP}_{\text{max}}$  (Adjusted  $R^2 = 0.666$ ,  $p = 0.001$ ),  $\Delta$  area under the recruitment curve (Adjusted  $R^2 = 0.649$ ,  $p = 0.001$ ), and  $\Delta$  peak slope (Adjusted  $R^2 = 0.313$ ,  $p = 0.034$ ), while  $\Delta$  RMT did not reach significance (Adjusted  $R^2 = 0.204$ ,  $p = 0.079$ ). Stepwise linear regression identified  $\Delta \text{MEP}_{\text{max}}$  as the most significant predictor of reduced net metabolic power during motor adaptation ( $\Delta$  net metabolic power  $= 0.161 + 0.875 * \Delta \text{MEP}_{\text{max}}$ ,  $\text{AIC} = -38.35$ , model  $p = 0.021$ ). Together, these results suggest that TMS indices of CSE were significant predictors of the decrease in net metabolic power that accompanies spatiotemporal adaptation during motor adaptation.

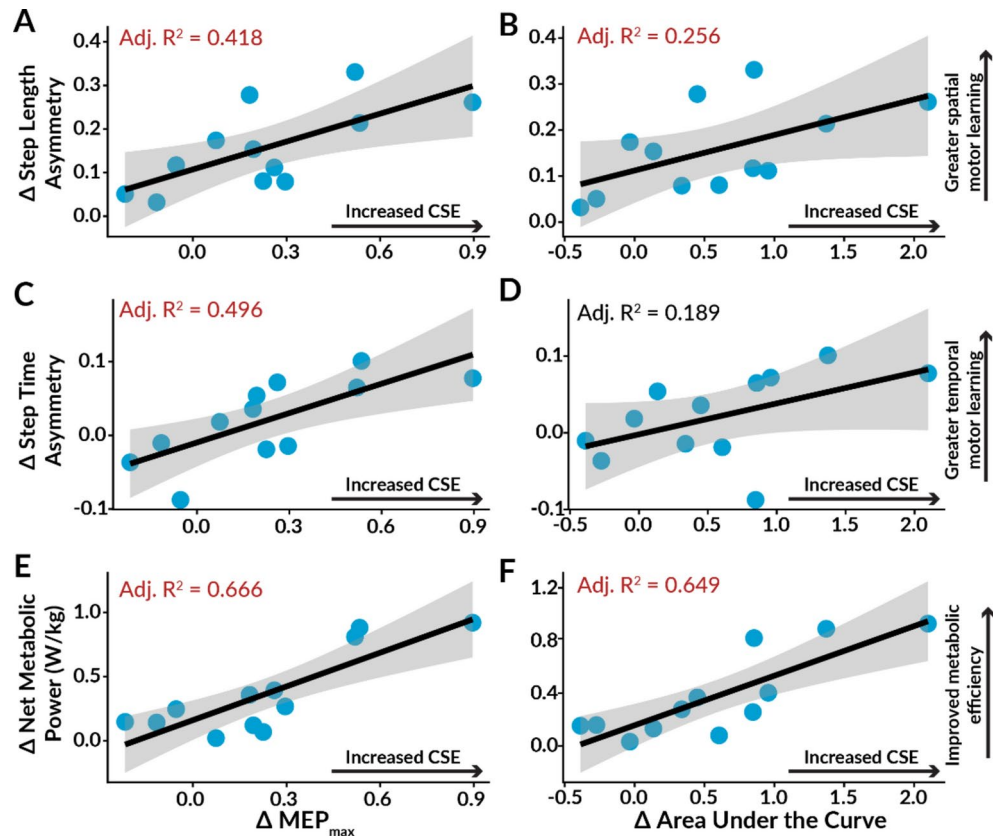


**Fig. 5.** Linear regressions among TMS indices of AIH-induced enhancements in corticospinal excitability and their correlation with motor adaptation outcomes. The red text indicates statistically significant adjusted  $R^2$  values ( $p < 0.05$ ), while the black text signifies insignificant values. (A) We observed a significant positive correlation between increased maximum motor-evoked potential amplitude ( $MEP_{max}$ ) post-AIH and improvements in step length asymmetry during Adapt 1. (B) The association between elevated area under the recruitment curve post-AIH and enhanced step length asymmetry during motor adaptation did not reach statistical significance ( $p = 0.053$ ). (C) We identified a significant correlation between elevated  $MEP_{max}$  post-AIH and augmented step time asymmetry during Adapt 1. (D). Correlations between increased area under the recruitment curve post-AIH and greater step time asymmetry during motor adaptation did not reach statistical significance ( $p = 0.088$ ). (E) Elevated  $MEP_{max}$  after AIH exhibited a positive correlation with decreased net metabolic power during motor adaptation. (F) Heightened area under the recruitment curve post-AIH positively correlated with reduced net metabolic power during Adapt 1. Individual data points are represented in blue, and the 95% confidence interval is illustrated by the grey-shaded area.

### Motor savings: spatiotemporal asymmetry

We characterized motor savings following AIH by quantifying the magnitude of spatiotemporal adaptation retained during initial Adapt 2 compared to initial Adapt 1 (Fig. 6A-C)<sup>37</sup>. We observed significant savings of spatial symmetry, as evidenced by more symmetric step lengths during initial Adapt 2 relative to initial Adapt 1 ( $t(11) = -4.46$ ,  $p < 0.001$ ) and during late Adapt 2 relative to late Adapt 1 ( $t(11) = -4.70$ ,  $p < 0.001$ ). Additionally, we found significant savings of both STA and DSA. STA was significantly higher during initial Adapt 2 compared to initial Adapt 1 ( $t(11) = -2.35$ ,  $p = 0.039$ ), as well as from late Adapt 2 compared to late Adapt 1 ( $t(11) = -2.41$ ,  $p = 0.035$ ). For DSA, Tukey's post-hoc comparisons identified significantly lower asymmetry during initial Adapt 2 compared to initial Adapt 1 ( $t(11) = 4.43$ ,  $p = 0.001$ ) and from late Adapt 2 compared to late Adapt 1 ( $t(11) = 3.02$ ,  $p = 0.012$ ). Therefore, participants displayed motor savings of both spatial and temporal parameters of adaptation.

### Motor savings: net metabolic power

We assessed savings of metabolic adaptation by comparing net metabolic power during early Adapt 2 to early Adapt 1 (Fig. 6D). Tukey's pairwise comparisons indicated significantly lower net metabolic power during early Adapt 2 compared to early Adapt 1 ( $t(11) = 3.75$ ,  $p = 0.003$ ), demonstrating that participants retained improved metabolic efficiency. The mean net metabolic power during early Adapt 2 was 5.39 W/kg (SD = 1.13), with a 0.7 W/kg reduction compared to early Adapt 1.

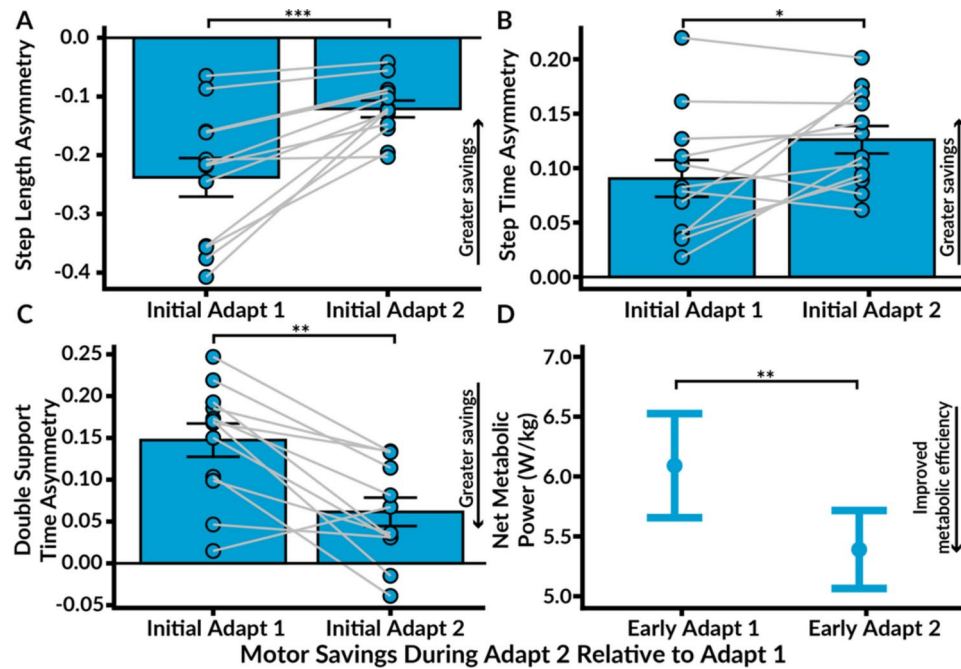


**Fig. 6.** Motor Savings. We characterized motor savings by measuring the degree of spatiotemporal adaptation from initial Adapt 1 to initial Adapt 2 and the extent of metabolic adaptation from early Adapt 1 to early Adapt 2. **(A)** Savings of step length asymmetry were evidenced by significantly lower asymmetry during initial Adapt 2 relative to initial Adapt 1. **(B)** Step time asymmetry was significantly elevated during initial Adapt 2 compared to initial Adapt 1. **(C)** Savings of double support time asymmetry were observed, as asymmetry was significantly lower during initial Adapt 2 compared to initial Adapt 1. **(D)** Savings of improved metabolic efficiency were also shown by lower net metabolic power during Adapt 2 compared to Adapt 1. The bars represent standard error. Significance levels are denoted as \*\*\* $p < 0.001$ , \*\* $p < 0.01$ , and \* $p < 0.05$ .

### Lower limb excitability predicts motor savings: spatiotemporal asymmetry

To evaluate how well  $\Delta \text{MEP}_{\text{max}}$ ,  $\Delta$  area under the recruitment curve,  $\Delta$  peak slope, and  $\Delta$  RMT explained the variance in motor savings outcomes, we conducted linear regression analyses and computed adjusted  $R^2$  values (Fig. 7, Supplementary Table S2).

A significant positive correlation was observed between elevated  $\text{MEP}_{\text{max}}$  following AIH and the savings of lower SLA (Adjusted  $R^2 = 0.625$ ,  $p = 0.001$ ). Furthermore, the increased area under the recruitment curve positively correlated with the savings of lower SLA (Adjusted  $R^2 = 0.290$ ,  $p = 0.041$ ). Stepwise linear regression identified  $\Delta \text{MEP}_{\text{max}}$  and  $\Delta$  peak slope as the two best predictors of SLA savings ( $\Delta \text{SLA} = 0.053 + 0.416 * \Delta \text{MEP}_{\text{max}} - 0.366 * \Delta$  peak slope,  $\text{AIC} = -75.05$ , model  $p = 0.005$ ,  $\text{MEP}_{\text{max}}$   $p = 0.002$ , slope  $p = 0.0423$ ), explaining 77.33% of the variance.

Linear regression analyses also revealed a significant positive correlation between increased  $\text{MEP}_{\text{max}}$  after AIH and the savings of elevated STA (Adjusted  $R^2 = 0.538$ ,  $p = 0.004$ ). Additionally, we observed a significant positive correlation between the elevated area under the recruitment curve and the savings of higher STA (Adjusted  $R^2 = 0.307$ ,  $p = 0.036$ ). Stepwise linear regression indicated that both  $\Delta \text{MEP}_{\text{max}}$  and  $\Delta$  peak slope were the primary predictors of STA savings ( $\Delta \text{STA} = 0.002 + 0.203 * \Delta \text{MEP}_{\text{max}} - 0.152 * \Delta$  peak slope,  $\text{AIC} = -79.24$ , model  $p = 0.065$ ,  $\text{MEP}_{\text{max}}$   $p = 0.039$ , peak slope  $p = 0.261$ ).

Both the  $\Delta \text{MEP}_{\text{max}}$  and  $\Delta$  peak slope explained 49.03% of the variance in STA savings. However, no significant correlations were observed between any of the TMS indices and the savings of lower DSA (model  $p = 0.468$ ). These results suggest that TMS indices of CSE were strong predictors of the degree of motor savings observed for both SLA and STA.

### Lower limb excitability predicts motor savings: net metabolic power

Net metabolic power exhibited a robust positive correlation with  $\Delta \text{MEP}_{\text{max}}$  (Adjusted  $R^2 = 0.645$ ,  $p = 0.001$ ),  $\Delta$  the area under the recruitment curve (Adjusted  $R^2 = 0.693$ ,  $p < 0.001$ ), and  $\Delta$  peak slope (Adjusted  $R^2 = 0.406$ ,  $p = 0.015$ ), with  $\Delta$  RMT not reaching significance ( $p = 0.065$ ). Stepwise linear regression analysis identified  $\Delta$  area under the recruitment curve as the best predictor of net metabolic power savings ( $\Delta$  net metabolic power  $= 0.251 + 0.776 * \Delta$  area under the recruitment curve,  $\text{AIC} = -22.76$ , model  $p = 0.024$ ). Overall, we found that TMS indices representing changes in CSE post-AIH significantly predicted the savings of lower net metabolic power upon subsequent split-belt walking exposures.



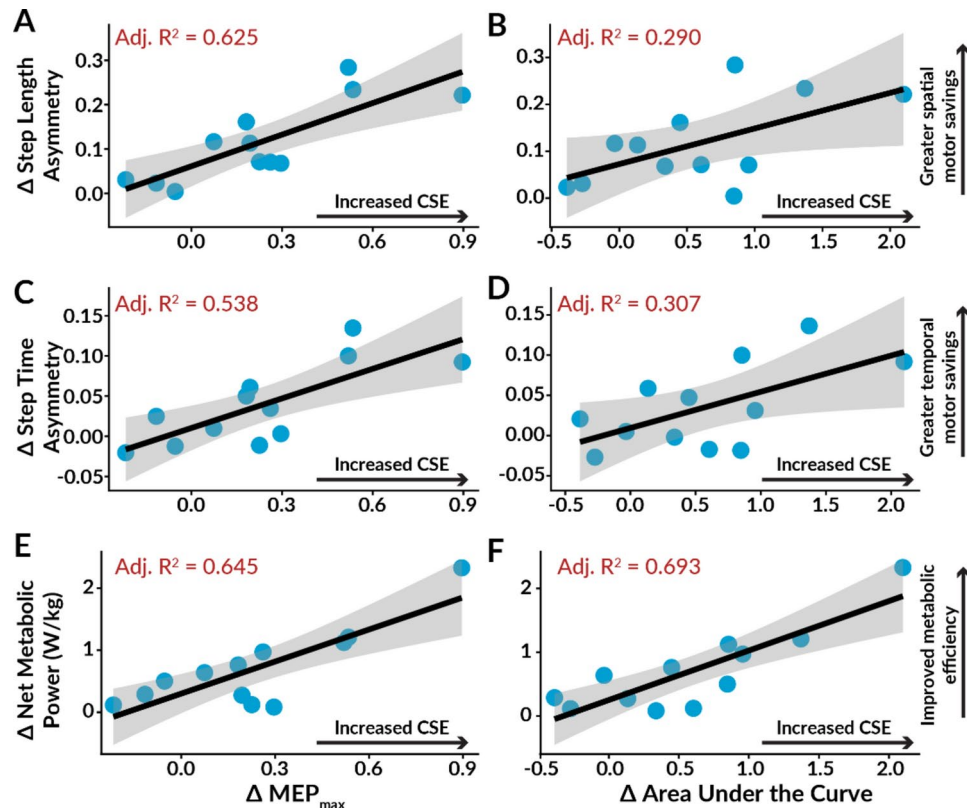


**Fig. 7.** Linear regressions among indices of AIH-induced enhancements in corticospinal excitability and their correlation with motor savings outcomes. The red text indicates statistically significant adjusted  $R^2$  values ( $p < 0.05$ ), while the black text signifies insignificant values. (A) We identified a significant correlation between increased maximum motor-evoked potential amplitude ( $MEP_{max}$ ) after AIH and savings of lower step length asymmetry. (B) Increased area under the recruitment curve post-AIH exhibited a significant correlation with the savings of lower step length asymmetry. (C) We observed a significant correlation between heightened  $MEP_{max}$  post-AIH and the savings of higher step time asymmetry. (D) Increased area under the recruitment curve post-AIH positively correlated with the savings of higher step time asymmetry. (E) There was a significant correlation between elevated  $MEP_{max}$  after AIH and the savings of lower net metabolic power. (F) We found a positive correlation between a larger area under the recruitment curve post-AIH and the savings of lower net metabolic power. Individual data points are shown in blue, and the 95% confidence interval is represented by the grey-shaded area.

### Spatiotemporal asymmetry predicts net metabolic power

Both  $\Delta$  SLA and  $\Delta$  STA significantly correlated with  $\Delta$  net metabolic power during motor adaptation ( $\Delta$  SLA Adjusted  $R^2 = 0.452$ ,  $p = 0.010$ ;  $\Delta$  STA Adjusted  $R^2 = 0.396$ ,  $p = 0.017$ ) and motor savings ( $\Delta$  SLA Adjusted  $R^2 = 0.461$ ,  $p = 0.009$ ;  $\Delta$  STA Adjusted  $R^2 = 0.468$ ,  $p = 0.008$ ). In contrast,  $\Delta$  DSA did not correlate with  $\Delta$  net metabolic power (motor adaptation  $p = 0.734$ ; motor savings  $p = 0.580$ ). While changes in spatiotemporal asymmetry significantly predicted improvements in metabolic efficiency (Supplementary Fig. S3), changes in  $MEP_{max}$  and the area under the recruitment curve explained a greater portion of the variance in net metabolic power.

### Retrospective comparison of learning between a mild vs. large perturbation

To better understand how perturbation size affects motor adaptation and motor savings after AIH, we retrospectively compared the degree of spatiotemporal and metabolic adaptation between a large 1:2 belt speed ratio and a milder 1:1.5 belt speed ratio reported in Bogard et al. 2023 (See Fig. 1A and Supplementary Fig. S4). The results of the statistical tests are summarized in Supplementary Table S5. Briefly, Tukey's post-hoc analyses indicated that the large perturbation group achieved more symmetrical step lengths during both motor adaptation and motor savings compared to the mild perturbation group. The average decrease in SLA for the large perturbation group was 0.09 lower during motor adaptation ( $SD = 0.15$ ) and 0.07 lower during motor savings ( $SD = 0.15$ ) than the mild perturbation group. The large perturbation group also demonstrated greater motor savings of STA, maintaining an average STA that was 0.04 higher than the mild perturbation group ( $SD = 0.09$ ). Both the mild and large perturbation groups displayed similar magnitudes of motor adaptation and motor savings of DSA. The large perturbation group exhibited greater savings of improved metabolic efficiency, with net metabolic power that was an average of 0.57 W/kg lower than the mild perturbation group ( $SD = 0.96$ ). Although we did not find a significant group difference in net metabolic power during motor adaptation, the

large perturbation group averaged 0.35 W/kg lower than the mild perturbation group (SD = 0.96). Overall, the larger perturbation led to greater motor adaptation of SLA and more prominent motor savings of SLA, STA, and metabolic efficiency.

## Discussion

Our results provide the first evidence that TA excitability is amplified after 5 days of AIH. In support of our hypothesis, changes in TA excitability are positively correlated with both improved motor adaptation and motor savings. Furthermore, our study demonstrates a novel association between elevated lower limb excitability and greater metabolic efficiency. Together, these results indicate that both changes in excitability and reductions in net metabolic power are markers of AIH-mediated neuroplasticity.

### AIH Increases lower limb excitability

Our results advance the understanding of AIH-induced neuroplasticity beyond the upper limb by demonstrating that TA area under the recruitment curve, MEP<sub>max</sub>, and MEP amplitudes at both 120% and 140% of RMT are elevated following repetitive AIH, but not SHAM. Additionally, our study did not detect any concurrent changes in the maximal voluntary contraction, aligning with prior able-bodied research<sup>13,39</sup>. This suggests that changes in maximal voluntary contraction may not parallel changes in net descending and spinal excitability in able-bodied individuals. However, this observation contrasts that observed in individuals with iSCI<sup>1,40,41</sup>, who often exhibit deficits in voluntary muscle activation<sup>42</sup>.

The composite nature of MEPs precludes the differentiation of the specific contributions of neural pathways, including cortical networks, descending tracts, spinal circuits, thalamic relays, and brainstem or cerebellar inputs, to behavioral outcomes<sup>43</sup>. Rather, our collective findings indicate that AIH increases net motoneuronal excitability. Indeed, our recent work observed a significant increase in voluntary activation of ankle muscles during repeated contractions following repetitive AIH without any concurrent changes in  $H_{max}/M_{max}$ , further supporting the notion of increased descending neural drive<sup>13</sup>. Prior research on the upper limb has shown increases in both CSE and spike-timing-dependent plasticity after a single AIH session, whereas measures of intracortical inhibition and facilitation remained unchanged<sup>9</sup>. Together with our observations suggest that AIH enhances net motoneuronal excitability.

Notably, inconsistent findings have been reported regarding the effect of a single AIH session on CSE, which may be partially attributed to variations in dosing. For instance, compared to Christiansen et al. (2018) and our study, Finn et al. (2022) only observed increased CSE at discrete time points while utilizing a more conservative desaturation threshold of 75% and omitting the remaining hypoxic interval. In contrast, Radia et al. (2022) implemented a longer 3-min hypoxic interval and did not detect changes in CSE. Notably, we observed significant increases in CSE after multiple-day AIH administration, utilizing dosing intervals that conferred improvements in walking performance after iSCI<sup>2,3</sup>. Given the distinct cortical representations of upper and lower limb muscles<sup>44</sup> and the varying motor thresholds required to evoke MEPs in these regions<sup>45</sup>, direct comparisons between our findings and AIH studies on upper limb muscles should be made cautiously. These factors, along with functional differences between hand and ankle muscles, may contribute to differences in the magnitude of AIH-induced changes across motoneuron pools. Nevertheless, our findings of increased TA excitation after repetitive AIH suggest potential applications in neurorehabilitation to promote adaptive neuroplasticity.

### Lower limb excitability predicts motor adaptation and motor savings

To our knowledge, this is the first study to examine the functional significance of changes in CSE following repetitive AIH in humans. We demonstrate that the degree of CSE enhancement post-AIH predicts gains in motor adaptation, as evidenced by a positive correlation between increased MEP<sub>max</sub> and greater spatiotemporal adaptation. Additionally, increased MEP<sub>max</sub> and area under the recruitment curve post-AIH both correlate with larger savings of spatiotemporal adaptation. We argue for the interpretation that enhanced CSE is not only a marker of AIH-mediated neuroplasticity but also supports the processes that underlie the acquisition and savings of new motor skills. This is supported by preceding investigations that have linked CSE to improvements in both visuomotor adaptation<sup>46,47</sup> and savings of visuomotor adaptation<sup>19,48</sup>.

Although heightened CSE may support motor learning processes, it is important to acknowledge that able-bodied individuals can still acquire new motor skills without changes<sup>32,37</sup> or even with decreases in CSE<sup>49</sup>. Indeed, we observed that participants with no changes or decreases in CSE still successfully adapted spatiotemporal coordination, albeit to a lesser extent (Fig. 5). It is also possible that increased motor adaptation after AIH<sup>14</sup> contributes to the observed increases in CSE<sup>19,20</sup>. However, it is unlikely that improvements in motor adaptation alone facilitate increases in CSE as motor training paradigms show that elevated CSE only persists with additional task challenges<sup>22,50</sup>. Furthermore, we evaluated changes in CSE prior to assessing motor adaptation, minimizing the potential influence of learning-related processes on CSE measurements. This assessment was conducted within a conservative 75-min window, consistent with prior studies demonstrating that CSE remains elevated for up to 75 min following a single dose of AIH<sup>9</sup>. While we did not assess longer-term changes in CSE, our findings suggest that increases in CSE following repetitive AIH are closely associated with improvements in motor adaptation and motor savings.

Of particular interest is that we characterized improvements in motor adaptation and motor savings without any concurrent motor training paradigm. Previous work in humans demonstrated that AIH paired with task-specific motor training further amplifies walking performance after iSCI compared to AIH or training alone<sup>2,3</sup>. Motor training may further potentiate AIH-induced neuroplasticity through additive effects, as longitudinal human studies have shown that progressively challenging motor training enhances both motor learning and CSE<sup>22,51</sup>. This interaction may reflect shared mechanisms of actions that optimize neuroplasticity.

### Enhanced excitability predicts greater reductions in net metabolic power

Our findings reveal an unprecedented positive correlation between increased CSE and improved metabolic efficiency for both motor adaptation and motor savings. Specifically, increased MEP<sub>max</sub> area under the recruitment curve, and peak slope all positively correlate with reduced net metabolic power. Therefore, improved metabolic efficiency could serve as a marker of AIH-induced neuroplasticity. This interpretation is supported by our previous study, where the AIH group displayed lower net metabolic power at the start of the novel task and uniquely demonstrated significant savings of improved metabolic efficiency<sup>14</sup>.

Considering that improved metabolic efficiency is a feature of gains in motor adaptation<sup>52</sup>, it is plausible that the reductions in net metabolic power are primarily driven by improvements in spatiotemporal adaptation. Prior studies suggest that decrements in net metabolic power can persist beyond the plateau of biomechanical adaptations<sup>52,53</sup>, indicating that metabolic efficiency during motor adaptation is multifaceted. However, we observed a strong correlation between TMS indices of CSE and greater reductions in net metabolic power. Together, these observations indicate that metabolic efficiency cannot be explained by changes in biomechanics alone<sup>54</sup> and that net metabolic power provides an additional marker of AIH-mediated neuroplasticity.

### Potential mechanisms of increased CSE

Evidence from rodent models suggests that BDNF-dependent mechanisms play a central role in AIH-mediated neuroplasticity<sup>4–6</sup>. Therefore, it is plausible that BDNF may serve as the intermediary link between increments in CSE and enhancements in motor learning. Prior investigations in exercise-dependent increases in BDNF<sup>55</sup> substantiate this interpretation by showing concomitant increases in CSE and motor learning<sup>15</sup>. Conversely, individuals with a BDNF val66met polymorphism, known to decrease activity-dependent BDNF secretion, do not exhibit a significant change in CSE following a complex motor task<sup>56</sup>, whereas increasing CSE through motor cortex stimulation enhances motor learning<sup>16</sup>.

While our study did not assess the involvement of BDNF, its established role in contributing to energy efficiency<sup>57</sup> by promoting synaptic plasticity<sup>58</sup> and corticospinal synaptogenesis<sup>59</sup> could suggest that heightened CSE after AIH may facilitate BDNF-mediated energy efficiency. Critical for this interpretation, the AIH-dependent upregulation of BDNF has been shown to strengthen excitatory glutamatergic synapses in rodents with iSCI<sup>60</sup>. Importantly, rodents with increased BDNF signaling demonstrate increased excitatory neurotransmission and plasticity<sup>61</sup>. In humans, genetic disruption of BDNF impairs the formation of excitatory glutamatergic synapses<sup>62</sup>. Future studies are needed to clarify the role of BDNF in regulating metabolic efficiency in humans.

### Larger perturbations may promote better motor savings

While our previous study revealed significant improvements in motor adaptation and savings after AIH at a mild perturbation<sup>14</sup>, it remains unclear whether higher levels of task difficulty differentially facilitate motor adaptation and savings after AIH. Prior work found that continuously increasing the task difficulty drives persistent increases in CSE<sup>22</sup>. Additionally, earlier studies have demonstrated that greater challenges, such as larger split-belt speed perturbations, result in enhanced motor adaptation and savings<sup>37</sup>. Consistent with earlier findings<sup>37</sup>, we observed greater motor adaptation and savings of SLA with the large perturbation. Notably, we also observed greater savings of higher STA and improved metabolic efficiency with the large perturbation. Our findings suggest that greater challenges lead to more substantial enhancements in both motor adaptation and metabolic efficiency. Tailoring task difficulty has the potential to optimize rehabilitation strategies post-AIH.

### Limitations

This study provides novel insights into the role of AIH-induced neuroplasticity in motor adaptation and motor savings, though several limitations should be considered. First, we examined whether CSE changes on day 5 correlated with improvements in spatiotemporal adaptation and savings given our previous findings that 5 days of AIH enhances both motor adaptation and motor savings<sup>14</sup>. We utilized the same AIH dosing and duty cycle as previous studies that demonstrated cumulative benefits for walking performance in iSCI populations<sup>2,3,7</sup>. However, the current study design cannot differentiate whether the observed increase in CSE on day 5 resulted from cumulative exposure or was driven primarily by an acute response from the final AIH exposure.

Another consideration is how natural CSE fluctuations over time may influence our results. Prior research indicates that measures of CSE to the TA are consistent across days<sup>63</sup>, with strong test–retest reliability<sup>64</sup>. To limit confounding factors that may influence CSE variability across days, participants maintained their regular activity levels and diets. We excluded individuals undergoing physical therapy or new training programs. The absence of CSE changes in the SHAM group further supports that the observed CSE facilitation likely results from repetitive AIH rather than time-related factors or repeated testing.

We also recognize that the relationship between CSE and motor learning is both task<sup>29,30</sup> and learning modality-dependent<sup>43</sup>. While studies have demonstrated an association between corticospinal drive and motor adaptation<sup>25,65</sup>, CSE changes are more commonly linked to improvements in ballistic<sup>66</sup> and visuomotor tasks<sup>19,20,23</sup>. Interpreting variations in MEP amplitudes is also complex, as larger MEP responses do not directly equate to better motor learning outcomes<sup>43</sup>. Indeed, motor adaptation can occur with stable or even reduced CSE<sup>49</sup>. This suggests that while CSE facilitation may enhance motor adaptation or motor savings post-AIH, it is not a prerequisite for learning.

Finally, to ensure that participants were naïve to split-belt perturbation, we assessed their adaptation only post-AIH. Evidence shows that able-bodied individuals retain walking symmetry for up to three weeks without further practice<sup>67</sup>, making a pre-post design unsuitable for assessing motor adaptation using a split-belt walking paradigm. Because our study focused on the relationship between CSE changes and enhanced motor adaptation post-AIH<sup>14</sup>, we did not measure motor adaptation in the SHAM group. Future research should examine the

time course of CSE facilitation during repetitive AIH to clarify the potential effect of meta-plasticity on motor function.

In conclusion, our study not only uncovers the positive effects of repetitive AIH on lower limb excitability but also establishes its critical role in predicting motor adaptation, motor savings, and metabolic efficiency. Optimizing motor learning to drive gains in motor function after neurological injury necessitates a closer examination of the interplay between AIH-induced corticospinal plasticity and the structure of motor training during rehabilitation.

## Methods

### Participants

Twenty-six able-bodied subjects between the ages of 18 to 65 participated in the study at the University of Colorado, Boulder. An a priori analysis using G\*Power (v3.1.9.6) indicated that a sample size of 12 participants would be suitable to detect significant within-group differences in corticospinal excitability (CSE) between pre- and post-measures ( $t(10.5)=1.80$ , effect size=0.80, power=0.80, alpha=0.05). Therefore, data were initially collected from 13 participants assigned to the AIH group as part of a pre-post study design (Females=7; Mean age=23.4 ± 1.8 years; Mean height=173.6 ± 9.4 cm; Mean weight=72.6 ± 17.0 kg). To serve as a control, an additional 13 participants were subsequently recruited and assigned to a blinded normoxia SHAM group (Females=6; Mean age=23.2 ± 3.9 years; Mean height=174.4 ± 9.5 cm; Mean weight=72.9 ± 17.0 kg). A second a priori analysis indicated that a sample size of 10.5 participants per group would be sufficient to examine between-group changes in CSE ( $t(38.1)=1.69$ , effect size=0.80, power=0.80, alpha=0.05). As a result, group assignment was not randomized. The demographic characteristics of both groups are summarized in Supplementary Table S6.

Inclusion criteria included healthy able-bodied individuals aged 18 to 65 years old with no known history of neurological injury. Exclusion criteria comprised a history of cardiovascular disease, pulmonary complications, pain, syncope, sensitivity to altitude, or currently pregnant or undergoing physical therapy. All participants provided written informed consent before participation. All experimental procedures were approved by the Colorado Multiple Institutional Review Board (COMIRB #20-0689). The study adhered to the principles of the Declaration of Helsinki, and registration was completed at clinicaltrials.gov (NCT05341466; 22/04/2022).

### Experimental design

The experimental design is illustrated in Fig. 1A. Subjects visited the laboratory for five consecutive days to participate in experiments, receiving either five days of AIH or SHAM. On the first day, we assessed baseline TA excitability using TMS before administering the first dose of AIH or SHAM ('pre-TMS'). Following the pre-TMS session, participants received AIH or SHAM for five consecutive days at the same time each day. A cover was placed over the Hypoxico generator to further ensure participant blindness, despite previous work demonstrating that participants cannot distinguish between AIH and SHAM<sup>68</sup>. SpO<sub>2</sub> was monitored at 1 Hz for participant safety.

Two trained operators manually regulated the supply of low-oxygen air (AIH) or blinded normoxia (SHAM) by connecting a hose to a non-rebreather mask<sup>31</sup>. Each AIH dose entailed 15 cycles, each comprised of 90-s intervals of breathing low-oxygen air (9% ± 2% O<sub>2</sub>) alternated with 60-s intervals of breathing ambient air (21% ± 2% O<sub>2</sub>)<sup>3</sup>. The SHAM group received 90-s intervals of normoxia (21% ± 2% O<sub>2</sub>)<sup>3</sup>. We recorded oxygen saturation (SpO<sub>2</sub>) and heart rate (HR) at 1 Hz while blood pressure (BP) was measured every five cycles (Masimo; Irvine, CA). We paused the hypoxic interval if SpO<sub>2</sub> fell below 70%, HR exceeded 160 bpm or systolic BP went above 160 mmHg and resumed once SpO<sub>2</sub> returned above 80%, HR dropped below 140 bpm, and systolic BP decreased below 140 mmHg. The experiment terminated if the participant reported pain, dizziness, diaphoresis, tinnitus, or blurred vision. All participants tolerated AIH without meeting any of the predetermined safety criteria.

On the last day, participants underwent a second TMS session within 15 min after completing their final dose of AIH or SHAM ('post-TMS'). The split-belt walking task was performed following the second TMS session to ensure that motor adaptation did not influence CSE.

### Transcranial magnetic stimulation protocol

To examine alterations in resting CSE, we utilized monophasic, single-pulse TMS (DuoMAG MP-Dual Magnetic Stimulator; Deymed, Czechia) to target the leg motor area of the primary motor cortex<sup>69</sup>. We positioned an insulated, double-cone coil (DuoMAG Butterfly V-Shaped Coil; Deymed, Czechia) 0–2 cm posterior to the vertex to evoke MEPs in the TA muscle, targeting the region that obtained the lowest threshold and shortest latency response<sup>70</sup> recorded via surface electromyography (EMG) (Bipolar Ag/AgCl, spaced 22 mm apart, Noraxon Inc., USA). Notably, resting TA MEPs are highly reproducible<sup>71</sup> and the TA requires a lower stimulus intensity than other ankle muscles<sup>72</sup>. Prior studies have established a close link between corticospinal drive and TA excitability<sup>73</sup>. Additionally, enhancing TA excitability holds clinical significance as the TA MEP amplitude positively correlates with the magnitude of foot clearance during the swing phase of walking after iSCI<sup>24</sup>.

We utilized a generic brain MRI scaled to anatomical references and an NDI Polaris Vicra camera for real-time navigation of the TMS coil (Visor2, ANT-NeuroNav, Netherlands). The hotspot was defined as the stimulation vector where the largest MEP could be evoked in the TA with the lowest stimulation intensity<sup>74</sup>. The resting motor threshold (RMT) was then determined as the lowest stimulus intensity to elicit at least 4 MEPs ≥ 50 µV out of 7 trials over the hotspot. We used 7 trials as a conservative intermediary between the commonly used 5-trial criterion<sup>75</sup> and the 10-trial criterion<sup>76</sup>.

Recruitment curves were generated by plotting the peak-to-peak amplitudes of the TA MEPs against their corresponding normalized stimulus intensities, expressed as a percentage of RMT from 90 to 140% RMT. To



compare changes in CSE across participants and testing sessions pre- to post-intervention, we normalized the recruitment curves to the RMT during each respective testing session<sup>11</sup>. Thus, the recruitment curve sampling involved a pseudo-randomized sequence of stimulations ranging from 90 to 140% of the RMT<sup>77,78</sup>, with 6 pulses applied per intensity (Signal; CED, UK)<sup>79</sup>. We delivered TMS stimuli in 15-s intervals with a 15% time variation to prevent synaptic fatigue and minimize MEP variability<sup>80</sup>.

### Split-belt walking protocol

During the split-belt walking protocol, participants learned to walk on treadmill belts set at different speeds (D-flow v3.34.3; Motek, Netherlands). We secured participants into a passive safety harness and instructed them to refrain from using the handrails. To prevent inadvertent stepping onto the contralateral treadmill belt, participants were permitted to observe their feet in a mirror<sup>14</sup>.

The split-belt walking protocol comprised of four walking conditions: (1) 'Baseline', with matched belt speeds set at 1 m/s for 300 strides, (2) 'Adapt 1', involving a 2:1 split-belt speed ratio for 300 strides, (3) 'Washout', with tied-belts set at 1 m/s for 350 strides, and (4) 'Adapt 2', replicating the 2:1 split-belt speed ratio for 300 strides<sup>37</sup>. The perturbed belt was randomized<sup>81</sup>. Importantly, participants remained unaware that the leg perturbed during the split-belt walking protocol corresponded to the same leg used for recording surface EMG during the TMS protocol. We increased the belt speed 15–30 strides into the adaptation condition to blind the subjects to the timing<sup>14</sup>.

### Data collection

#### *Electromyography*

We placed bipolar Ag/AgCl electrodes, spaced 22 mm apart, over the TA, one-third of the distance from the fibular head to the lateral malleolus, and a ground electrode over the patella (Noraxon Inc., USA)<sup>42</sup>. To obtain low impedance ( $< 5 \text{ k } \Omega$ ), we first shaved and cleaned the skin with an isopropyl alcohol wipe<sup>82</sup>. EMG signals were bandpass filtered within a range of 20–1000 Hz, amplified by a gain 100 (CED 1902), sampled at 10 kHz (CED 1401), and displayed in real-time using Signal software (CED, UK). We outlined the electrode placement to reproduce the position post-intervention.

#### *Maximal voluntary contraction*

Prior to each TMS session, participants were instructed to generate three, 5-s maximal dorsiflexion contractions against a resistive load, with a minimum 1-min rest between trials<sup>83</sup>. We directed participants to contract their TA as forcefully and rapidly as possible without engaging their thigh muscles<sup>84</sup>. If the maximal peak-to-peak amplitude varied by more than 10%, the participant performed additional contractions<sup>85</sup>. We defined the maximal voluntary contraction (MVC) as the highest value obtained using EMG. A repeated measures ANOVA did not show a main effect of Timepoint (pre vs. post;  $F(1) = 0.00$ ,  $p = 1.00$ ), MVC number (MVC 1 vs. MVC 2 vs. MVC 3;  $F(2) = 0.051$ ,  $p = 0.95$ ), or an interaction effect between the two ( $F(2) = 0.00$ ,  $p = 1.00$ ), indicating repeated MVCs did not induce fatigue.

#### *Kinematics*

A 10-camera motion system captured lower limb kinematic data at a sampling frequency of 100 Hz (Vicon Nexus v2.8.1; Vicon Motion Systems, UK). We bilaterally placed reflective markers over the shank and thigh, as well as on the anterior and posterior superior iliac spines, iliac crests, greater trochanters, medial and lateral femoral epicondyles, medial and lateral malleoli, calcanei, and first and fifth metatarsal heads<sup>14</sup>. We analyzed kinematic data using custom pipelines in Visual3D (v2021.11.3; C-motion Inc., MD) and MATLAB (R2023b; MathWorks, Inc., US).

#### *Kinetics*

Three-dimensional ground reaction forces (GRF) were collected at a sampling frequency of 1000 Hz (D-flow v3.34.3; Motek, Netherlands) and low-pass filtered with a fourth-order Butterworth filter at a cutoff frequency of 20 Hz<sup>86</sup>. We used GRFs to validate gait events.

#### *Expired gas analysis*

We measured the rate of oxygen consumption ( $\text{VO}_2$ ) and carbon dioxide production ( $\text{VCO}_2$ ) using open circuit spirometry (TrueOne 2400; ParvoMedics Inc., UT). Resting metabolic rate was estimated based on the average  $\text{VO}_2$  and  $\text{VCO}_2$  of the last 2 min of a 5-min standing trial and was subtracted from the subsequent net metabolic power measured during walking<sup>32</sup>. The mean resting metabolic rate was 1.42 W/kg (SD = 0.18). Respiratory exchange ratios (RER;  $\text{VCO}_2/\text{VO}_2$ ) below 1 indicated predominant utilization of aerobic pathways<sup>53</sup>.

### Data analysis

#### *Maximum motor evoked potential*

The MEP onset was identified using custom configurations in Signal (CED, UK) as the first frame at which the peak-to-peak amplitude exceeded three standard deviations of the background EMG<sup>71</sup> recorded 200 ms preceding the TMS stimuli<sup>33</sup>. To account for the pre-stimulus baseline TA activation, we subtracted the mean background EMG from all MEPs<sup>34</sup>. We averaged the peak-to-peak MEP amplitudes across all participants and quantified the change in  $\text{MEP}_{\text{max}}$  pre- and post-intervention ( $\Delta \text{MEP}_{\text{max}}$ ). We additionally report raw MEP amplitudes normalized to the RMT of the corresponding testing session, as well as MEP amplitudes expressed as a percentage of baseline values.

#### Area under the recruitment curve

We calculated the area under the recruitment curve both pre- and post-intervention ( $\Delta$  area under the recruitment curve) using the trapezoidal method of area estimation. The area under the recruitment curve provides a crude measure of overall net excitability from 90 to 140% of RMT<sup>87</sup>.

#### Recruitment curve slope

The recruitment curve slope was determined by fitting a Boltzmann distribution in MATLAB using the Levenberg–Marquardt algorithm, as shown in Eq. 1.<sup>88</sup> The Boltzmann equation is a function of stimulus intensity ( $s$ ) and response amplitude (MEP), where  $MEP_{max}$  is the maximum averaged response from the recruitment curve,  $s_{50}$  is the stimulus intensity required to produce a response with half the amplitude of  $MEP_{max}$ , and  $k$  is the slope parameter<sup>89</sup>.

$$MEP(s) = \frac{MEP_{max}}{1 + e^{(s_{50}-s)/k}} \quad (1)$$

Peak slope, the inverse of the slope parameter, represents the rate of the MEP increase relative to  $MEP_{max}$  and is used to quantify the change in the gain of excitability<sup>78</sup>. We calculated alterations in peak slope pre- and post-intervention ( $\Delta$  peak slope).

#### Resting motor threshold

RMT represents the motor threshold required to excite the TA at rest<sup>74</sup>. We compared the RMT before and after AIH or SHAM ( $\Delta$  RMT).

#### Spatiotemporal asymmetry

We identified heel-strike and toe-off gait events for each stride using a vertical GRF detection threshold of 30 N<sup>90</sup>. These gait events were utilized to calculate step length asymmetry (SLA), step time asymmetry (STA), and double support time asymmetry (DSA). Step lengths and step times were determined by the fore-aft contralateral calcanei markers at heel-strike, while double support times were defined as the duration between the leading limb's heel-strike and contralateral toe-off<sup>87</sup>. We computed asymmetry values using Eq. 2,<sup>91</sup> where values of 0 indicate perfect symmetry.

$$\text{Asymmetry} = \frac{\text{Fast leg} - \text{Slow leg}}{\text{Fast leg} + \text{Slow leg}} \quad (2)$$

The phases 'initial learning' and 'late learning' were defined as the first five strides after the speed perturbation and the final twenty strides, respectively<sup>37</sup>. We assessed motor adaptation by examining the magnitude of spatiotemporal adaptation from initial Adapt 1 to late Adapt 1 and motor savings by the extent of adaptation from initial Adapt 1 to initial Adapt 2. Enhanced motor adaptation and motor savings were characterized by reductions in SLA and DSA towards symmetry values of 0, coupled with augmentations in STA towards positive asymmetry. This is supported by extensive research demonstrating these adaptation patterns in able-bodied individuals<sup>37,38,92</sup>. Given evidence of a distinct mode-dependency in the neural control of split-belt walking compared to split-belt running<sup>93</sup>, we excluded one participant from gait analyses due to utilizing a running strategy with a distinct aerial phase during both Adapt 1 and Adapt 2.

#### Net metabolic power

We quantified metabolic power using a standard regression Eq. 94. The mean resting metabolic rate was subtracted from metabolic power and then normalized to body mass to compute net metabolic power (W/kg)<sup>95</sup>. We omitted the first minute of each condition to account for the time lag of the expired gas reaching the mixing chamber<sup>14</sup>. Thus, we defined 'early' and 'late' net metabolic power as the second and last minute of each condition, respectively<sup>32</sup>. We characterized the extent of metabolic changes during motor adaptation by assessing the difference in net metabolic power from early Adapt 1 to late Adapt 1. Additionally, we characterized metabolic savings by comparing early Adapt 1 and early Adapt 2.

#### Retrospective comparisons

To gain deeper insights into how perturbation size affects AIH-induced enhancements in motor adaptation and motor savings, we conducted a retrospective analysis comparing the magnitude of spatiotemporal and metabolic adaptation between a large 1:2 belt speed ratio and a milder 1:1.5 belt speed ratio. The spatiotemporal and metabolic data for the large perturbation size were collected as part of the present study, while the corresponding data for the mild perturbation size were obtained from Bogard et al. (2023). The mild perturbation group comprised the AIH group reported in Bogard et al. (2023) ( $N=15$ ). Evidence suggests that increasing task difficulty can improve subsequent motor learning<sup>37,51</sup> and potentiate cortical plasticity<sup>22</sup>. Thus, the primary objective of this analysis was to determine whether AIH further enhances motor adaptation and motor savings under greater challenges, considering its demonstrated efficacy even under mild challenges<sup>14</sup>. Determining specific split-belt walking parameters that optimize motor adaptation and motor savings will clarify our understanding of the effects of AIH on motor adaptation.

#### Statistical analysis

Statistical analyses of the experimental data were conducted in R Studio (v2021.09.0) with a significance level set at  $p < 0.05$ . Group data are presented as mean  $\pm$  standard deviation (SD) in the text. We evaluated normality using

the Shapiro-Wilks test, multicollinearity using the variance of inflation factor, and sphericity using Mauchly's Test.

#### *Background EMG*

To evaluate the consistency of the pre-stimulus background EMG between pre- and post-TMS sessions, we conducted a paired t-test.

#### *TA excitability*

We assessed normality with the Shapiro-Wilk test, homogeneity with Levene's test, and sphericity with Mauchly's test. We utilized linear mixed model ANOVAs to analyze changes in area under the recruitment curve, incorporating fixed effects for timepoint (pre, post), group (AIH, SHAM), and their interaction, with a random intercept to account for variability across participants. We performed a Wilcoxon rank sum exact test to examine group differences (AIH vs. SHAM) in MEP as a percentage of baseline values, as well as an independent t-test to assess whether differences in MEP<sub>max</sub> were significantly different than baseline MEP<sub>max</sub>. We also assessed alterations in TA excitability pre- and post-intervention using paired t-tests for normally distributed data and Wilcoxon signed-rank tests when normality assumptions were not met. In addition, we conducted a repeated measures ANOVA with the Greenhouse-Geisser degrees of freedom correction to compare the peak-to-peak MEP amplitude pre- and post-intervention at the stimulus intensities of 100% RMT, 120% RMT, and 140% RMT, with the within-factors of 'stimulus intensity' (100%, 120%, and 140% RMT) and 'timepoint' (pre- and post-intervention). We conducted post hoc analyses utilizing Tukey's honest significant difference method to correct for multiple comparisons.

#### *Bayesian Hierarchical Modeling*

To assess whether background EMG influenced MEP amplitudes in the AIH group, we employed a Bayesian hierarchical model. Given the nonlinear relationship between background EMG and MEP amplitude, we log-transformed MEP amplitudes prior to analysis<sup>35</sup>. The model included log-transformed MEP amplitude as the outcome variable, with timepoint (pre-AIH vs. post-AIH) and background EMG as fixed effects, and a random intercept for participant identifier to account for repeated measures. We used weakly informative normal priors (mean = 0, SD = 1) for the fixed effects, reflecting an assumption of no strong effect unless supported by the data<sup>36</sup>. Residual variance was modeled using a Student's t-distribution (degrees of freedom = 3, mean = 0, scale = 2.5) to enhance robustness against outliers.

Model estimation was conducted using Markov Chain Monte Carlo (MCMC) sampling with four chains, each running for 4,000 iterations (2000 warm-up, 2000 sampling). Convergence was evaluated using the potential scale reduction factor ( $\hat{R}$ ), where values equal to 1 indicate well-mixed chains. Effective sample size (ESS) was computed for both bulk and tail distributions to ensure adequate posterior sampling. Parameters exceeding 1000 samples indicated reliable estimates. Model fit was validated through posterior predictive checks, comparing simulated data to observed values to ensure accurate representation of variability in MEP amplitudes.

Bayesian hypothesis testing evaluated: (1) whether post-AIH MEP amplitudes were higher than pre-AIH MEP amplitudes when controlling for background EMG, and (2) whether background EMG contributed to MEP amplitudes when controlling for timepoint. Posterior estimates were summarized using the posterior mean ( $\beta$ ), 95% credible interval (CI), posterior probability, and evidence ratio (ER). A 95% CI excluding zero was interpreted as strong evidence for an effect. The posterior probability quantified the certainty that the effect was in the expected direction, with values near 1 (100%) indicating high certainty. The ER quantified how much more likely the tested hypothesis was compared to the null hypothesis ( $\beta \leq 0$ ).

To further examine the influence of background EMG, we compared models with and without background EMG as a predictor using leave-one-out cross-validation (LOO-CV)<sup>96</sup>. We report the expected log predictive density (ELPD) difference and standard error, where a small ELPD difference indicates that including background EMG does not meaningfully improve model accuracy. Additionally, we report Bayesian  $R^2$  to estimate the proportion of variance in log-transformed MEP amplitudes explained by each model, with similar  $R^2$  values indicating a negligible predictive contribution of background EMG.

#### *Adaptation*

We conducted a two-way ANOVA to investigate the main effects of the within-factors 'condition' and 'learning phase' on spatiotemporal asymmetry (SLA, STA, DSA) and net metabolic power. We treated the subject identification number as a random factor to acknowledge that the same participants were measured across different levels of the within-subject factors, contributing to a repeated measures design. Assumptions of sphericity were not violated for any of the dependent variables; thus, corrections were not applied. Subsequently, we conducted two Tukey's post-hoc tests for each ANOVA to explore any potential significant pairwise comparisons. We used Tukey's pairwise comparisons to analyze motor adaptation of spatiotemporal symmetry between initial Adapt 1-late Adapt 1 and initial Adapt 2-late Adapt 2. Additionally, comparisons were made between early Adapt 1-late Adapt 1 to evaluate metabolic adaptation. We also performed Tukey's pairwise comparisons between initial Adapt 1-initial Adapt 2 and late Adapt 1-late Adapt 2 to assess savings of spatiotemporal adaptation, as well as between early Adapt 1-early Adapt 2 to examine savings of metabolic efficiency.

#### *Correlations*

We performed linear regression analyses between TMS indices of CSE and motor adaptation outcomes, as well as between TMS indices of CSE and motor savings outcomes. To compare how well TMS indices of CSE explained the variance in net metabolic power compared to parameters of spatiotemporal asymmetry, we also performed linear regression analyses with  $\Delta$  SLA,  $\Delta$  STA, and  $\Delta$  DSA as the predictors and  $\Delta$  net metabolic power as the

outcome variable. We calculated the adjusted  $R^2$  values for each linear regression to measure the proportion of the variance in behavior explained by changes in CSE. In addition, we used stepwise linear regression models to iteratively eliminate insignificant predictor variables. For each model, the predictor variables were  $\Delta \text{MEP}_{\text{max}}$ ,  $\Delta$  area under the recruitment curve,  $\Delta$  peak slope, and  $\Delta$  RMT, and the dependent variables were the motor adaptation and motor savings outcomes ( $\Delta$  SLA,  $\Delta$  STA,  $\Delta$  DSA, and  $\Delta$  net metabolic power). The final stepwise linear regression model was determined based on achieving the lowest Akaike information criterion (AIC) and highest adjusted  $R^2$  value.

#### Retrospective comparisons

We compared motor adaptation and motor savings between a mild and a large perturbation. To address differences in sample size, we utilized linear mixed models, incorporating Satterthwaite's method for estimating degrees of freedom. Subsequently, we used an ANOVA to assess significance, with perturbation size as the between-group factor (1:1.5 belt speed ratio and 1:2 belt speed ratio) and adaptation period as the within-group factor ( $\Delta$  motor adaptation and  $\Delta$  motor savings). Significant ANOVAs were followed by Tukey's post-hoc analysis to adjust for multiple comparisons.

#### Data availability

The authors confirm that the data supporting the findings of this study are fully available and presented in the supporting information of the manuscript. Correspondence and requests for materials should be addressed to A.Q.T.

Received: 12 April 2024; Accepted: 17 February 2025

Published online: 24 February 2025

#### References

- Trumbower, R. D., Jayaraman, A., Mitchell, G. S. & Rymer, W. Z. Exposure to acute intermittent hypoxia augments somatic motor function in humans with incomplete spinal cord injury. *Neurorehabil Neural Repair* **26**, 163–172 (2012).
- Hayes, H. B. et al. Daily intermittent hypoxia enhances walking after chronic spinal cord injury: A randomized trial. *Neurology* **82**, 104–113 (2014).
- Tan, A. Q., Sohn, W. J., Naidu, A. & Trumbower, R. D. Daily acute intermittent hypoxia combined with walking practice enhances walking performance but not intralimb motor coordination in persons with chronic incomplete spinal cord injury. *Exper. Neurol.* **340**, 113669 (2021).
- Baker-Herman, T. L. et al. BDNF is necessary and sufficient for spinal respiratory plasticity following intermittent hypoxia. *Nat. Neurosci.* **7**, 48–55 (2004).
- Satriotomo, I. et al. Repetitive acute intermittent hypoxia increases growth/neurotrophic factor expression in non-respiratory motor neurons. *Neuroscience* **322**, 479–488 (2016).
- Lovett-Barr, M. R. et al. Repetitive intermittent hypoxia induces respiratory and somatic motor recovery after chronic cervical spinal injury. *J. Neurosci.* **32**, 3591–3600 (2012).
- Navarrete-Opazo, A., Alcayaga, J., Sepúlveda, O., Rojas, E. & Astudillo, C. Repetitive intermittent hypoxia and locomotor training enhances walking function in incomplete spinal cord injury subjects: A randomized, triple-blind Placebo-Controlled Clinical Trial. *J. Neurotrauma* **34**, 1803–1812 (2017).
- Spampinato, D. A., Ibanez, J., Rocchi, L. & Rothwell, J. Motor potentials evoked by transcranial magnetic stimulation: Interpreting a simple measure of a complex system. *J. Physiol.* **601**, 2827–2851 (2023).
- Christiansen, L., Urbin, M., Mitchell, G. S. & Perez, M. A. Acute intermittent hypoxia enhances corticospinal synaptic plasticity in humans. *eLife* **7**, e34304 (2018).
- Finn, H. T. et al. The effect of acute intermittent hypoxia on human limb motoneurone output. *Exper. Physiol.* **107**, 615–630 (2022).
- Radia, S. et al. Effects of acute intermittent hypoxia on corticospinal excitability within the primary motor cortex. *Eur. J. Appl. Physiol.* **122**, 2111–2123 (2022).
- Mathew, A. J., Finn, H. T., Carter, S. G., Gandevia, S. C. & Butler, J. E. Motor-evoked potentials in the human upper and lower limb do not increase after single 30-min sessions of acute intermittent hypoxia. *J. Appl. Physiol.* **137**, 51–62 (2024).
- Bogard, A. T., Pollet, A. K. & Tan, A. Q. Intermittent hypoxia enhances voluntary activation and reduces performance fatigability during repeated lower limb contractions. *J. Neurophysiol.* **132**, 1717–1728 (2024).
- Bogard, A. T., Hemmerle, M. R., Smith, A. C. & Tan, A. Q. Enhanced motor learning and motor savings after acute intermittent hypoxia are associated with a reduction in metabolic cost. *J. Physiol.* **602**, 5879–5899 (2023).
- Mang, C. S., Snow, N. J., Campbell, K. L., Ross, C. J. D. & Boyd, L. A. A single bout of high-intensity aerobic exercise facilitates response to paired associative stimulation and promotes sequence-specific implicit motor learning. *J. Appl. Physiol.* **117**, 1325–1336 (2014).
- Fritsch, B. et al. Direct current stimulation promotes BDNF-dependent synaptic plasticity: Potential implications for motor learning. *Neuron* **66**, 198–204 (2010).
- Joundi, R. A. et al. The effect of BDNF val66met polymorphism on visuomotor adaptation. *Exp. Brain Res.* **223**, 43–50 (2012).
- Helm, E. E., Tyrell, C. M., Pohlig, R. T., Brady, L. D. & Reisman, D. S. The presence of a single-nucleotide polymorphism in the BDNF gene affects the rate of locomotor adaptation after stroke. *Exp. Brain Res.* **234**, 341–351 (2016).
- Hirano, M., Kubota, S., Tanabe, S., Koizume, Y. & Funase, K. Interactions among learning stage, retention, and primary motor cortex excitability in motor skill learning. *Brain Stimul.* **8**, 1195–1204 (2015).
- Sarwary, A. M. E., Wischniewski, M., Schutter, D. J. L. G., Selen, L. P. J. & Medendorp, W. P. Corticospinal correlates of fast and slow adaptive processes in motor learning. *J. Neurophysiol.* **120**, 2011–2019 (2018).
- Cantarero, G., Lloyd, A. & Celnik, P. Reversal of long-term potentiation-like plasticity processes after motor learning disrupts skill retention. *J. Neurosci.* **33**, 12862–12869 (2013).
- Christiansen, L. et al. Long-term motor skill training with individually adjusted progressive difficulty enhances learning and promotes corticospinal plasticity. *Sci. Rep.* **10**, 15588 (2020).
- Bagce, H. F., Saleh, S., Adamovich, S. V., Krakauer, J. W. & Tunik, E. Corticospinal excitability is enhanced after visuomotor adaptation and depends on learning rather than performance or error. *J. Neurophysiol.* **109**, 1097–1106 (2013).
- Barthélemy, D. et al. Impaired transmission in the corticospinal tract and gait disability in spinal cord injured persons. *J. Neurophysiol.* **104**, 1167–1176 (2010).
- Sato, S. & Choi, J. T. Increased intramuscular coherence is associated with temporal gait symmetry during split-belt locomotor adaptation. *J. Neurophysiol.* **122**, 1097–1109 (2019).



26. Bawa, P., Chalmers, G. R., Stewart, H. & Eisen, A. A. Responses of ankle extensor and flexor motoneurons to transcranial magnetic stimulation. *J. Neurophysiol.* **88**, 124–132 (2002).
27. Cheney, P. D., Belhaj-Saïf, A. & Boudrias, M.-H. Principles of corticospinal system organization and function. In *Handbook of Clinical Neurophysiology* Vol. 4 59–96 (Elsevier, 2004).
28. Christiansen, L. et al. Acute intermittent hypoxia boosts spinal plasticity in humans with tetraplegia. *Exper. Neurol.* **335**, 113483 (2021).
29. Perez, M. A., Lungholt, B. K. S., Nyborg, K. & Nielsen, J. B. Motor skill training induces changes in the excitability of the leg cortical area in healthy humans. *Exp. Brain Res.* **159**, 197–205 (2004).
30. Dambreville, C., Neige, C., Mercier, C., Blanchette, A. K. & Bouyer, L. J. Corticospinal excitability quantification during a visually-guided precision walking task in humans: Potential for neurorehabilitation. *Neurorehabil. Neural Repair* **36**, 689–700 (2022).
31. Tan, A. Q., Papadopoulos, J. M., Corsten, A. N. & Trumbower, R. D. An automated pressure-swing absorption system to administer low oxygen therapy for persons with spinal cord injury. *Exper. Neurol.* **333**, 113408 (2020).
32. Finley, J. M., Bastian, A. J. & Gottschall, J. S. Learning to be economical: the energy cost of walking tracks motor adaptation: Split-belt adaptation reduces metabolic power. *J. Physiol.* **591**, 1081–1095 (2013).
33. Vargas, C. D. The influence of hand posture on corticospinal excitability during motor imagery: A transcranial magnetic stimulation study. *Cerebral Cortex* **14**, 1200–1206 (2004).
34. Diehl, Ph., Kliesch, U., Dietz, V. & Curt, A. Impaired facilitation of motor evoked potentials in incomplete spinal cord injury. *J. Neurol* **253**, 51–57 (2006).
35. Nielsen, J. F. Logarithmic distribution of amplitudes of compound muscle action potentials evoked by transcranial magnetic stimulation. *J. Clin. Neurophysiol.* **13**, 423–434 (1996).
36. Cai, Z., Pellegrino, G., Lina, J.-M., Benali, H. & Grova, C. Hierarchical Bayesian modeling of the relationship between task-related hemodynamic responses and cortical excitability. *Hum. Brain Mapp.* **44**, 876–900 (2023).
37. Leech, K. A., Roemmich, R. T. & Bastian, A. J. Creating flexible motor memories in human walking. *Sci. Rep.* **8**, 94 (2018).
38. Buurke, T. J. W., Lamothe, C. J. C., Vervoort, D., Van Der Woude, L. H. V. & Den Otter, R. Adaptive control of dynamic balance in human gait on a split-belt treadmill. *J. Exper. Biol.* <https://doi.org/10.1242/jeb.174896> (2018).
39. Tan, A. Q., Tuthill, C., Corsten, A. N., Barth, S. & Trumbower, R. D. A single sequence of intermittent hypoxia does not alter stretch reflex excitability in able-bodied individuals. *Exper. Physiol.* **109**, 576–587 (2024).
40. Sandhu, M. S. et al. Prednisolone pretreatment enhances intermittent hypoxia-induced plasticity in persons with chronic incomplete spinal cord injury. *Neurorehabil. Neural Repair* **33**, 911–921 (2019).
41. Lynch, M. et al. Effect of acute intermittent hypoxia on motor function in individuals with chronic spinal cord injury following ibuprofen pretreatment: A pilot study. *J. Spinal Cord Med.* **40**, 295–303 (2017).
42. Kim, H. E., Corcos, D. M. & Hornby, T. G. Increased spinal reflex excitability is associated with enhanced central activation during voluntary lengthening contractions in human spinal cord injury. *J. Neurophysiol.* **114**, 427–439 (2015).
43. Carson, R. G., Ruddy, K. L. & McNickle, E. What do TMS-evoked motor potentials tell us about motor learning? In *Advances in experimental medicine and biology* Vol. 957 (eds Laczo, J. & Latash, M. L.) 143–157 (Springer, 2016).
44. Proessel, F. et al. Mapping the homunculus: Agreement between fMRI and TMS-based motor cortex hand, trunk and leg representations. *Brain Stimulation* **14**, 1692–1693 (2021).
45. De Luca, C. J. & Hostage, E. C. Relationship between firing rate and recruitment threshold of motoneurons in voluntary isometric contractions. *J. Neurophysiol.* **104**, 1034–1046 (2010).
46. Miyaguchi, S. et al. Time course of bilateral corticospinal tract excitability in the motor-learning process. *Neurosci. Lett.* **711**, 134410 (2019).
47. Mooney, R. A., Cirillo, J. & Byblow, W. D. Neurophysiological mechanisms underlying motor skill learning in young and older adults. *Exp. Brain Res.* **237**, 2331–2344 (2019).
48. Centeno, C. et al. The effects of aging on cortico-spinal excitability and motor memory consolidation. *Neurobiol. Aging* **70**, 254–264 (2018).
49. Holland, L., Murphy, B., Passmore, S. & Yelder, P. Time course of corticospinal excitability changes following a novel motor training task. *Neurosci. Lett.* **591**, 81–85 (2015).
50. Jensen, J. L., Marstrand, P. C. D. & Nielsen, J. B. Motor skill training and strength training are associated with different plastic changes in the central nervous system. *J. Appl. Physiol.* **99**, 1558–1568 (2005).
51. Christiansen, L. et al. Progressive practice promotes motor learning and repeated transient increases in corticospinal excitability across multiple days. *Brain Stimul.* **11**, 346–357 (2018).
52. Sánchez, N., Simha, S. N., Donelan, J. M. & Finley, J. M. Using asymmetry to your advantage: Learning to acquire and accept external assistance during prolonged split-belt walking. *J. Neurophysiol.* **125**, 344–357 (2021).
53. Huang, H. J., Kram, R. & Ahmed, A. A. Reduction of metabolic cost during motor learning of arm reaching dynamics. *J. Neurosci.* **32**, 2182–2190 (2012).
54. Bogard, A. T. & Tan, A. Q. Author response to Panza et al. *The Journal of Physiology* (2024) <https://doi.org/10.1113/JP287844>.
55. Skriver, K. et al. Acute exercise improves motor memory: Exploring potential biomarkers. *Neurobiol. Learn. Memory* **116**, 46–58 (2014).
56. Cirillo, J., Hughes, J., Ridding, M., Thomas, P. Q. & Semmler, J. G. Differential modulation of motor cortex excitability in BDNF Met allele carriers following experimentally induced and use-dependent plasticity. *Eur. J. Neurosci.* **36**, 2640–2649 (2012).
57. Kowiański, P. et al. BDNF: A key factor with multipotent impact on brain signaling and synaptic plasticity. *Cell Mol. Neurobiol.* **38**, 579–593 (2018).
58. Mizui, T., Tanima, Y., Komatsu, H., Kumanogoh, H. & Kojima, M. The biological actions and mechanisms of brain-derived neurotrophic factor in healthy and disordered brains. *Neurosci. Med.* **5**, 183–195 (2014).
59. Sasaki, M. et al. BDNF-hypersecreting human mesenchymal stem cells promote functional recovery, axonal sprouting, and protection of corticospinal neurons after spinal cord injury. *J. Neurosci.* **29**, 14932–14941 (2009).
60. Golder, F. J. & Mitchell, G. S. Spinal synaptic enhancement with acute intermittent hypoxia improves respiratory function after chronic cervical spinal cord injury. *J. Neurosci.* **25**, 2925–2932 (2005).
61. Ameroso, D. et al. Astrocytic BDNF signaling within the ventromedial hypothalamus regulates energy homeostasis. *Nat. Metab.* **4**, 627–643 (2022).
62. Sonoyama, T. et al. Human BDNF/TrkB variants impair hippocampal synaptogenesis and associate with neurobehavioural abnormalities. *Sci. Rep.* **10**, 9028 (2020).
63. Brangaccio, J. A., Phipps, A. M., Gemoets, D. E., Sniffen, J. M. & Thompson, A. K. Variability of corticospinal and spinal reflex excitability for the ankle dorsiflexor tibialis anterior across repeated measurements in people with and without incomplete spinal cord injury. *Exp. Brain Res.* **242**, 727–743 (2024).
64. Caccchio, A., Cimini, N., Alosi, P., Santilli, V. & Marrelli, A. Reliability of transcranial magnetic stimulation-related measurements of tibialis anterior muscle in healthy subjects. *Clin. Neurophysiol.* **120**, 414–419 (2009).
65. Orban De Xivry, J.-J., Ahmadi-Pajouh, M. A., Harran, M. D., Salimpour, Y. & Shadmehr, R. Changes in corticospinal excitability during reach adaptation in force fields. *J. Neurophysiol.* **109**, 124–136 (2013).
66. Lundbye-Jensen, J., Petersen, T. H., Rothwell, J. C. & Nielsen, J. B. Interference in ballistic motor learning: Specificity and role of sensory error signals. *PLoS ONE* **6**, e17451 (2011).
67. Buurke, T. J. W. et al. Split-belt walking: An experience that is hard to forget. *Gait Posture* **97**, 184–187 (2022).

68. Barth, S., Slocum, C., Zafonte, R., Tan, A. & Trumbower, R. Blinding Integrity Analysis of a Randomized Clinical Trial to Test the Effects of Therapeutic Intermittent Hypoxia in Able-bodied Adults [Abstract]. *AAPM&R Annual Assembly* (2021).
69. Eisner-Janowicz, I., Chen, B., Sangari, S. & Perez, M. A. Corticospinal excitability across lower limb muscles in humans. *J. Neurophysiol.* **130**, 788–797 (2023).
70. Kesar, T. M., Stinear, J. W. & Wolf, S. L. The use of transcranial magnetic stimulation to evaluate cortical excitability of lower limb musculature: Challenges and opportunities. *RNN* **36**, 333–348 (2018).
71. Lewis, G. N., Signal, N. & Taylor, D. Reliability of lower limb motor evoked potentials in stroke and healthy populations: How many responses are needed?. *Clin. Neurophysiol.* **125**, 748–754 (2014).
72. Nielsen, J. B., Pyndt, H. S. & Petersen, N. T. Investigating human motor control by transcranial magnetic stimulation. *Exper. Brain Res.* **152**, 1–16 (2003).
73. Capaday, C., Lavoie, B. A., Barbeau, H., Schneider, C. & Bonnard, M. Studies on the corticospinal control of human walking I. Responses to focal transcranial magnetic stimulation of the motor cortex. *J. Neurophysiol.* **81**, 129–139 (1999).
74. Nardone, R. et al. Assessment of corticospinal excitability after traumatic spinal cord injury using MEP recruitment curves: a preliminary TMS study. *Spinal Cord* **53**, 534–538 (2015).
75. Fujiyama, H., Garry, M. I., Levin, O., Swinnen, S. P. & Summers, J. J. Age-related differences in inhibitory processes during interlimb coordination. *Brain Res.* **1262**, 38–47 (2009).
76. Greenhouse, I., King, M., Noah, S., Maddock, R. J. & Ivry, R. B. Individual differences in resting corticospinal excitability are correlated with reaction time and GABA content in motor cortex. *J. Neurosci.* **37**, 2686–2696 (2017).
77. Thomas, S. L. & Gorassini, M. A. Increases in corticospinal tract function by treadmill training after incomplete spinal cord injury. *J. Neurophysiol.* **94**, 2844–2855 (2005).
78. Potter-Baker, K. A. et al. Reliability of TMS metrics in patients with chronic incomplete spinal cord injury. *Spinal Cord* **54**, 980–990 (2016).
79. Iyer, P. C. & Madhavan, S. Characterization of stimulus response curves obtained with transcranial magnetic stimulation from bilateral tibialis anterior muscles post stroke. *Neurosci. Lett.* **713**, 134530 (2019).
80. Hassanzahraee, M., Zoghi, M. & Jaberzadeh, S. Longer transcranial magnetic stimulation intertrial interval increases size, reduces variability, and improves the reliability of motor evoked potentials. *Brain Connect.* **9**, 770–776 (2019).
81. Reisman, D. S., Block, H. J. & Bastian, A. J. Interlimb coordination during locomotion: What can be adapted and stored?. *J. Neurophysiol.* **94**, 2403–2415 (2005).
82. Billot, M., Duclay, J., Rigoard, P., David, R. & Martin, A. Antagonist muscle torque at the ankle interfere with maximal voluntary contraction under isometric and anisometric conditions. *Sci. Rep.* **12**, 20238 (2022).
83. Kesar, T. M. et al. Agonist-antagonist coactivation enhances corticomotor excitability of ankle muscles. *Neural Plast.* **2019**, 1–12 (2019).
84. Jayaraman, A. et al. Locomotor training and muscle function after incomplete spinal cord injury: Case series. *J. Spinal Cord Med.* **31**, 185–193 (2007).
85. Zewdie, E. T., Roy, F. D., Yang, J. F. & Gorassini, M. A. Facilitation of descending excitatory and spinal inhibitory networks from training of endurance and precision walking in participants with incomplete spinal cord injury. *Progr. Brain Res.* **218**, 127–1555 (2015).
86. Gottschall, J. S. & Kram, R. Energy cost and muscular activity required for propulsion during walking. *J. Appl. Physiol.* **94**, 1766–1772 (2003).
87. Kemlin, C. et al. Redundancy among parameters describing the input-output relation of motor evoked potentials in healthy subjects and stroke patients. *Front. Neurol.* **10**, 535 (2019).
88. Devanne, H., Lavoie, B. A. & Capaday, C. Input-output properties and gain changes in the human corticospinal pathway. *Exp. Brain Res.* **114**, 329–338 (1997).
89. Carroll, T. J., Riek, S. & Carson, R. G. Reliability of the input–output properties of the cortico-spinal pathway obtained from transcranial magnetic and electrical stimulation. *J. Neurosci. Methods* **112**, 193–202 (2001).
90. Karakasis, C. & Artemiadis, P. Real-time kinematic-based detection of foot-strike during walking. *J. Biomech.* **129**, 110849 (2021).
91. Stenum, J. & Choi, J. T. Step time asymmetry but not step length asymmetry is adapted to optimize energy cost of split-belt treadmill walking. *J. Physiol.* **598**, 4063–4078 (2020).
92. Malone, L. A., Bastian, A. J. & Torres-Oviedo, G. How does the motor system correct for errors in time and space during locomotor adaptation?. *J. Neurophysiol.* **108**, 672–683 (2012).
93. Ogawa, T., Kawashima, N., Obata, H., Kanosue, K. & Nakazawa, K. Mode-dependent control of human walking and running as revealed by split-belt locomotor adaptation. *J. Exper. Biol.* **218**, 3192–3198 (2015).
94. Péronnet, F. & Massicotte, D. Table of nonprotein respiratory quotient: an update. *Can. J. Sport Sci.* **16**, 23–29 (1991).
95. Sánchez, N., Park, S. & Finley, J. M. Evidence of energetic optimization during adaptation differs for metabolic, mechanical, and perceptual estimates of energetic cost. *Sci. Rep.* **7**, 7682 (2017).
96. Vehtari, A., Gelman, A. & Gabry, J. Practical Bayesian model evaluation using leave-one-out cross-validation and WAIC. *Stat. Comput.* **27**, 1413–1432 (2017).

## Acknowledgements

We would like to thank our study participants and our collaborators at the University of Colorado, Anschutz Medical Campus.

## Author contributions

A.T.B., T.G.H., A.C.S., and A.Q.T. contributed to the conception and design of the study; A.T.B., T.G.H., and A.K.P. conducted the experiments; A.T.B. and T.G.H. analyzed the data; A.T.B. and T.G.H. drafted the original manuscript; all authors contributed to the interpretation of the results and revisions of the manuscript; All authors approved the final version of the manuscript.

## Funding

AB Nexus Grant, NIH National Center of Neuromodulation for Rehabilitation, P2CHD086844. Eunice Kennedy Shriver National Institute of Child Health and Human Development of the National Institutes of Health, K01HD106928, Boettcher Foundation's Webb-Waring Biomedical Research Program.

## Declarations

## Competing interests

The authors declare no competing interests.

### Additional information

**Supplementary Information** The online version contains supplementary material available at <https://doi.org/10.1038/s41598-025-90890-8>.

**Correspondence** and requests for materials should be addressed to A.Q.T.

**Reprints and permissions information** is available at [www.nature.com/reprints](http://www.nature.com/reprints).

**Publisher's note** Springer Nature remains neutral with regard to jurisdictional claims in published maps and institutional affiliations.

**Open Access** This article is licensed under a Creative Commons Attribution-NonCommercial-NoDerivatives 4.0 International License, which permits any non-commercial use, sharing, distribution and reproduction in any medium or format, as long as you give appropriate credit to the original author(s) and the source, provide a link to the Creative Commons licence, and indicate if you modified the licensed material. You do not have permission under this licence to share adapted material derived from this article or parts of it. The images or other third party material in this article are included in the article's Creative Commons licence, unless indicated otherwise in a credit line to the material. If material is not included in the article's Creative Commons licence and your intended use is not permitted by statutory regulation or exceeds the permitted use, you will need to obtain permission directly from the copyright holder. To view a copy of this licence, visit <http://creativecommons.org/licenses/by-nc-nd/4.0/>.

© The Author(s) 2025